Atmos. Meas. Tech. Discuss., 8, 6599–6659, 2015
www.atmos-meas-tech-discuss.net/8/6599/2015/
doi:10.5194/amtd-8-6599-2015

Atmospheric Measurement Techniques Discussions
Open Access

EARLINET: potential operationality of a research network

M. Sicard[1,2], G. D'Amico[3], A. Comerón[1], L. Mona[3], L. Alados-Arboledas[4], A. Amodeo[3], H. Baars[5], L. Belegante[6], I. Binietoglou[6], J. A. Bravo-Aranda[7], A. J. Fernández[8], P. Fréville[9], D. García-Vizcaíno[1], A. Giunta[3], M. J. Granados-Muñoz[4], J. L. Guerrero-Rascado[4], D. Hadjimitsis[10], A. Haefele[11], M. Hervo[9], M. Iarlori[12], P. Kokkalis[13], D. Lange[1,2], R. E. Mamouri[10], I. Mattis[14], F. Molero[8], N. Montoux[9], A. Muñoz[1], C. Muñoz Porcar[1], F. Navas-Guzmán[15], D. Nicolae[6], A. Nisantzi[10], N. Papagiannopoulos[3], A. Papayannis[13], S. Pereira[16], J. Preißler[17], M. Pujadas[8], V. Rizi[12], F. Rocadenbosch[1,2], K. Sellegri[9], V. Simeonov[11], G. Tsaknakis[13], F. Wagner[14], and G. Pappalardo[3]

[1]Dept. of Signal Theory and Communications, Remote Sensing Lab. (RSLab), Universitat Politècnica de Catalunya, Barcelona, Spain
[2]Ciències i Tecnologies de l'Espai – Centre de Recerca de l'Aeronàutica i de l'Espai/Institut d'Estudis Espacials de Catalunya (CTE-CRAE/IEEC), Universitat Politècnica de Catalunya, Barcelona, Spain
[3]Istituto di Metodologie per l'Analisi Ambientale (CNR-IMAA), C. da S. Loja, 85050 Tito Scalo, Potenza, Italy
[4]Departamento de Física Aplicada, Universidad de Granada, Granada, Spain

[5]Leibniz Institute for Tropospheric Research, Leipzig, Germany
[6]National Institute of R&D for Optoelectronics, Magurele, Ilfov, Romania
[7]Laboratoire Meteorologie Dinamique (LMD), École Polytechnique, Palaiseau, France
[8]Centro de Investigaciones Energéticas, Medioambientales y Tecnológicas (CIEMAT), Madrid, Spain
[9]Observatoire de Physique du Globe, Laboratoire de Météorologie Physique (LaMP-CNRS) Clermont-Ferrand, France
[10]Cyprus University of Technology, Limassol, Cyprus
[11]Federal Office of Meteorology and Climatology MeteoSwiss, Switzerland
[12]CETEMPS, Dipartimento di Scienze Fisiche e Chimiche, Università degli Studi, L'Aquila, Italy
[13]Laser Remote Sensing Unit, Physics Dept., National Technical University of Athens, Greece
[14]Deutscher Wetterdienst, Observatorium Hohenpeißenberg, Hohenpeißenberg, Germany
[15]Institute of Applied Physics (IAP), University of Bern, Bern, Switzerland
[16]Évora Geophysics Center, University of Évora, Portugal
[17]Centre for Climate and Air Pollution Studies (C-CAPS), National University of Ireland Galway, University Road, Galway, Ireland

Received: 27 April 2015 – Accepted: 01 June 2015 – Published: 01 July 2015

Correspondence to: M. Sicard (msicard@tsc.upc.edu)

Published by Copernicus Publications on behalf of the European Geosciences Union.

Abstract

In the framework of ACTRIS summer 2012 measurement campaign (8 June–17 July 2012), EARLINET organized and performed a controlled exercise of feasibility to demonstrate its potential to perform operational, coordinated measurements and deliver products in near-real time. Eleven lidar stations participated to the exercise which started on 9 July 2012 at 06:00 UT and ended 72 h later on 12 July at 06:00 UT. For the first time the Single-Calculus Chain (SCC), the common calculus chain developed within EARLINET for the automatic evaluation of lidar data from raw signals up to the final products, was used. All stations sent in real time measurements of 1 h of duration to the SCC server in a predefined netcdf file format. The pre-processing of the data was performed in real time by the SCC while the optical processing was performed in near-real time after the exercise ended. 98 and 84 % of the files sent to SCC were successfully pre-processed and processed, respectively. Those percentages are quite large taking into account that no cloud screening was performed on lidar data. The paper shows time series of continuous and homogeneously obtained products retrieved at different levels of the SCC: range-square corrected signals (pre-processing) and daytime backscatter and nighttime extinction coefficient profiles (optical processing), as well as combined plots of all direct and derived optical products. The derived products include backscatter- and extinction-related Ångström exponents, lidar ratios and color ratios. The combined plots reveal extremely valuable for aerosol classification. The efforts made to define the measurements protocol and to configure properly the SCC pave the way for applying this protocol for specific applications such as the monitoring of special events, atmospheric modelling, climate research and calibration/validation activities of spaceborne observations.

AMTD
8, 6599–6659, 2015

EARLINET: potential operationality of a research network

M. Sicard et al.

1 Introduction

Atmospheric aerosols have important effects on life on Earth: they can be toxic, by composition or by structure (size or shape); they deteriorate visibility (haze and fog occurrence depends on aerosols); ecosystems are affected by significant mass transport; etc. They also have an effect on many areas of the atmospheric sciences: they influence atmospheric chemistry by providing reactive surfaces (stratospheric ozone depletion, summer smog); they affect the radiation budget and hence the temperature distribution within the atmosphere and on the ground, including change in spectral distribution; etc. In the three areas of climate, weather and air quality, the aerosol contribution is one of the most uncertain contributions. As an example, the aerosol radiative effects on climate (aerosol-radiation interactions (direct and semi-direct effects): the direct interaction of radiation with aerosol absorption and scattering properties, and aerosol-cloud interactions (indirect effects): modification of clouds formation and their properties by aerosols) are still estimated with very large uncertainties according to the Intergovernmental Panel on Climate Change (IPCC) (IPCC, 2014). In the area of air quality, chemistry transport models often use in situ surface measurements extrapolated to the vertical column when observations of the aerosol vertical distribution are missing. This leads to substantial uncertainties in the forecast of particulate matter (Sartelet et al., 2007; Roustan et al., 2010).

The difficulties in quantifying the aerosol contribution, not only locally but on a global scale, are due to:

- Their high variability in space and time and, as a consequence, on their non-localized distribution, mostly due to medium- and long-range transport and short mean life time.

- The geographical extension of the sources: some are localized, others are distributed over large volumes.

- The large number of processes that lead to their production.

AMTD
8, 6599–6659, 2015

- The numerous and heterogeneous processes through which aerosols can interact during their lifetime: nucleation, condensation, coagulation and deposition.

The lidar technique is a powerful tool to assess the aerosol stratification, i.e. the vertical structure of the aerosol layers (bottom, top and thickness). Combined backscatter and Raman lidar systems allow the retrieval of the aerosol optical properties (backscatter and extinction coefficients). Advanced lidar systems (see Sect. 2.3 for the definition) provide in addition aerosol microphysical properties (fine and coarse fraction of the extinction coefficient, effective radius, complex refractive index and single scattering albedo).

Ground-based lidar networks are especially valuable to get vertical profiling of aerosols at scales from regional to global. In an effort to facilitate knowledge and data exchange between lidar groups, the Global Atmosphere Watch (GAW) Aerosol Lidar Observation Network (GALION) was formed envisioning the cooperation among existing lidar networks and contributions from individual stations (Hoff et al., 2008). At present, GALION consists of 8 existing and developing networks (2 operative networks operating backscatter systems working on a 24/24 h, 7/7 days basis and 6 research networks) in different regions of the globe:

- the Asian Dust Network (AD-Net)
- the Latin American Lidar Network (LALINET)
- the Commonwealth of Independent States Lidar Network (CIS-LiNet)
- the European Aerosol Research Lidar Network (EARLINET)
- the Micro Pulse Lidar Network (MPLNET)
- the Network for the Detection of Atmospheric Composition Change (NDACC)
- the NOAA Cooperative Remote Sensing Science and Technology (CREST) Lidar network (CLN)

Discussion Paper | Discussion Paper | Discussion Paper | Discussion Paper |

AMTD
8, 6599–6659, 2015

EARLINET: potential operationality of a research network

M. Sicard et al.

– the Canadian Operational Research Aerosol Lidar Network (CORALNet).

Among those networks EARLINET is the only one operating a majority of advanced Raman systems (Pappalardo et al., 2014).

EARLINET (www.earlinet.org), established in 2000, is the first coordinated aerosol lidar network whose key goal is the provision of a comprehensive, quantitative, and statistically significant database on the spatial and temporal aerosol distribution on a continental scale (Bösenberg et al., 2001; Pappalardo et al., 2014). At present, the network includes 27 active stations distributed over Europe (Pappalardo et al., 2014). Lidar observations within the network are performed on a regular schedule of one daytime measurement per week around 12 solar time, when the boundary layer is usually well developed, and two night time measurements per week, with low background light, in order to perform Raman extinction measurements. In addition to the routine measurements, further observations are devoted to monitoring of special events such as desert dust outbreaks (e.g. Ansmann et al., 2003; Mona et al., 2006; Papayannis et al., 2008; Guerrero-Rascado et al., 2008, 2009; Mamouri et al., 2013; Nisantzi et al., 2015), forest fires (e.g., Müller et al., 2007a; Amiridis et al., 2009; Alados-Arboledas et al., 2011; Nisantzi et al., 2014), photochemical smog (Carnuth et al., 2002), and volcanic eruptions (e.g., Pappalardo et al., 2004a, 2013; Wang et al., 2008; Mattis et al., 2010; Ansmann et al., 2010; Groß et al., 2011; Papayannis et al., 2012; Sicard et al., 2012; Navas-Guzmán et al., 2013). In June 2006 EARLINET started correlative measurements for the space-borne lidar on board of CALIPSO (Cloud-Aerosol Lidar and Infrared Pathfinder Satellite Observation) (Pappalardo et al., 2010). Although EARLINET was not conceived as an operational network, it already proved its capability of providing data in near-real time under special circumstances (Pappalardo et al., 2013). On the other hand, coordinated observations with data delivered in near-real time are of prime importance in the areas of weather and air quality and also for the monitoring of plumes from special events. The GAW Report No. 178 (2007) states, referring to lidar products: "For assimilation into chemical weather forecast models excellent temporal coverage, high reliability, and near real time delivery are the key properties requested".

In July 2012 EARLINET performed a controlled exercise of feasibility to demonstrate its potential to perform operational, coordinated measurements. To this aim the Single-Calculus Chain (SCC), the common calculus chain developed within EARLINET for the automatic evaluation of lidar data from raw signals up to the final products (D'Amico et al., 2012, 2015a, b; Mattis et al., 2015), was used for the first time in an automated way. The amount and the quality of the data obtained during the exercise, as well as the lessons learnt from it, offer promising perspectives for applications such as climate research (model evaluation, aerosol transport and tracers, impact on radiation), air quality (assessment and forecast) and the monitoring of plumes from special events.

The objective of this paper is to demonstrate the capabilities of the research network EARLINET to perform operational, coordinated measurements and deliver lidar products in near-real time. The paper deals first with logistic and technical issues (organization, measurements protocol, data harmonization) and then presents a global overview of the aerosol loading during the exercise in terms of lidar products obtained either in real or in near-real time as an illustration of the new perspectives that, through this exercise, EARLINET can offer to the modeling community and monitoring agencies. The paper is organized as follows: it describes the organization of the exercise and the systems involved in Sect. 2; Sect. 3 gives the four-dimensional (4-D) evolution of the aerosol layers observed during the exercise and presents some potential applications making use of the data obtained. Conclusions are given in Sect. 5.

2 Campaign setup and systems

2.1 Campaign motivation and setups

Two of the most challenging objectives of the exercise in terms of operationality were (1) to perform continuous measurements during a relatively long period of time and to deliver raw data in real time, and (2) to run automatically in real time for the first time the SCC. In that sense a special effort was made to operate the systems taking into account that EARLINET lidar stations are mostly formed by research systems that currently operate neither automatically nor unmanned. A strong coordination effort was also made to harmonize the operational scheme, as well as data products and name conventions, to provide homogeneous documentation for systems and data and to establish common access points for the data.

The time window for starting the operationality exercise was fixed between 2 and 12 July 2012, while its duration was fixed to 3 complete days, i.e. 72 h, in order to fall within ACTRIS (Aerosols, Clouds, and Trace Gases Research Infrastructure Network) summer 2012 measurement campaign (8 June–17 July 2012) aimed mainly at the study of Saharan dust. The ACTRIS campaign gave support to two international field campaigns during summer 2012:

- The European Monitoring and Evaluation Programme (EMEP) (Espen Yttri et al., 2012) and
- the Chemistry-Aerosol Mediterranean Experiment (ChArMEx) (Dulac et al., 2012).

In order to optimize the chances to have a particularly interesting situation (such as an intrusion of Saharan dust or high levels of PM_{10}), weather prediction models, forecast models of dust such as NAAPS (Navy Aerosol Analysis and Prediction System; Christensen, 1997), Skiron (Nickovic et al., 2001) and BSC-DREAM8b (Barcelona Supercomputing Center – Dust Regional Atmospheric Model; Pérez et al., 2006a, b; Basart et al., 2012) and air quality models were consulted prior to launch the experiment.

2.2 Measurements protocol

The measurements protocol was defined on the basis of the ongoing EARLINET regular measurements (Pappalardo et al., 2009) and refined to fulfill the exercise objectives:

- Duration of the measurement per recorded file: 60 min.

AMTD
8, 6599–6659, 2015

- Raw temporal resolution: a number that 30 min. should be a multiple of in order to guarantee a minimum integration time of 30 min. for all systems.
- Range resolution: the system raw resolution.
- All wavelengths available should be recorded.
- No cloud screening is performed by the stations. Instead, each station is responsible for providing information about the maximum height (m a.s.l.) up to which the profile is cloud free.
- Strict and accurate synchronization of all stations to [hh]:[mm = 00 ± 1].
- Creation of one single netcdf file of the raw signals (power) per measurement.
- Upload to the SCC central server.

A first test of the operationality exercise took place on 23 April 2012, in which the stations of Granada, Barcelona, L'Aquila and Potenza participated. It lasted 10 h between 07:00 and 17:00 UT. Broken clouds were present above all the stations and intermittent rain also occurred over Italy. The objective of the test was to check the correct functioning of the measurement protocol, the data format of all systems and the reliability of the automatic pre-processing of the SCC. The pre-processed files were delivered by the SCC within a few minutes after the measurements ended. A total of 33 files were sent to the SCC that pre-processed successfully 27 of them (84 %).

2.3 Lidar systems

Eleven EARLINET stations around the Mediterranean Basin decided to participate to the exercise. From west to east (see Fig. 1 and Table 1):

- EV, Évora, Portugal (7.911° W, 38.568° N, 290 m a.s.l.)
- MA, Madrid, Spain (3.730° W, 45.450° N, 663 m a.s.l.)

AMTD
8, 6599–6659, 2015
EARLINET: potential operationality of a research network
M. Sicard et al.

- GR, Granada, Spain (3.610° W, 37.160° N, 680 m a.s.l.)
- BA, Barcelona, Spain (2.112° E, 41.389° N, 115 m a.s.l.)
- CL, Clermont-Ferrand, France (3.111° E, 45.761° N, 420 m a.s.l.)
- PA, Payerne, Switzerland (6.943° E, 46.813° N, 491 m a.s.l.)
- LA, L'Aquila, Italy (13.350° E, 42.368° N, 656 m a.s.l.)
- PO, Potenza, Italy (15.720° E, 40.600° N, 760 m a.s.l.)
- AT, Athens, Greece (23.780° E, 37.960° N, 212 m a.s.l.)
- BU, Bucharest, Romania (26.029° E, 44.348° N, 93 m a.s.l.)
- LM, Limassol, Cyprus (33.040° E, 34.640° N, 8 m a.s.l).

Seven stations operated an advanced lidar system (green labels in Fig. 1). Advanced lidars consist of at least 3 elastic wavelengths and 2 Raman wavelengths and allow for aerosol typing and microphysics retrieval. Four stations operated a Raman lidar system (orange labels in Fig. 1). Raman lidars consist of at least 1 elastic wavelength and 1 Raman wavelength and allow for the retrieval of the extinction and the backscatter coefficients at 1 wavelength. Six stations also performed measurements of the linear particle depolarization ratio at one elastic wavelength. Even though Payerne performed the measurements during the whole campaign, their data are not presented in this work because of a lack of manpower to follow on with the analysis of their data.

Figure 1 also indicates the stations where a sun-photometer is co-located. In total eight stations have also a co-located sun-photometer, all of them being part of the Aerosol Robotic Network (AERONET) (Holben et al., 1998). Sun-photometers allow for the retrieval of columnar values of parameters such as the aerosol optical depth (AOD), the Ångström exponent, the single scattering albedo or the size distribution among others. Sun-photometers are also a precious cooperative instrument to lidars

Discussion Paper | Discussion Paper | Discussion Paper | Discussion Paper |

AMTD

8, 6599–6659, 2015

EARLINET: potential operationality of a research network

M. Sicard et al.

for constraining elastic lidar inversions (Landulfo et al., 2003; Reba et al., 2010) and for microphysics retrieval (Wagner et al., 2013; Chaikovsky et al., 2015; Binietoglou et al., 2015).

The data quality of all EARLINET systems is assured by inter-comparisons at instrument level using transportable reference systems (Matthias et al., 2004; Sicard et al., 2009; Freudenthaler et al., 2010; Molero et al., 2012; Wandinger et al., 2015). The data quality assurance also includes the inter-comparison of elastic and Raman retrieval algorithms of each individual station (Böckmann et al., 2004; Pappalardo et al., 2004b; Sicard et al., 2009). Based on well-defined common standards and internal quality tests, the routinely performed quality-assurance exercises of lidar systems and algorithms ensure that the data products provided by the individual stations are homogenous and continuously of highest possible reliability (Freudenthaler, 2015). Efforts to improve the data quality derived from EARLINET observations are ongoing (Freudenthaler et al., 2010, 2015; Belegante et al., 2015; Engelmann et al., 2015; Bravo-Aranda et al., 2015; Amodeo et al., 2015).

2.4 The single-calculus chain

The Single Calculus Chain (SCC) is the standard tool for the automatic analysis of EARLINET data. It has been designed to provide quality assured aerosol products (according to EARLINET quality assurance program) starting from the raw lidar time series. Two different levels of quality assured products are made available: pre-processed range corrected signals and aerosol extinction and/or backscatter coefficients. The SCC is highly configurable and flexible to assure the automatic analysis of data coming from different type of lidars and, even for the same instrument, from different configurations. The SCC is composed by two independent but interconnected calculus modules: the EARLINET Lidar Pre-Processor (ELPP) module providing the pre-processed range corrected signals corrected for instrumental effects and the EARLINET Lidar Data Analyzer (ELDA) for the calculation of the aerosol optical products from the ELPP outputs. All the input parameters needed for the lidar analysis are collected in a database and

AMTD
8, 6599–6659, 2015

EARLINET: potential operationality of a research network

M. Sicard et al.

organized in terms of different lidar configurations. The modules ELPP and ELDA are automatically started and monitored by a dedicated daemon module when there are available input data not yet analyzed. The SCC is installed on a common server accessible by all EARLINET stations through a web interface which improves the user friendliness of the SCC. All the details of the SCC modules are described in this special issue (D'Amico at al., 2015a, b; Mattis et al., 2015).

For the exercise the SCC was configured to provide two kinds of aerosol products:

- SCC-1: pre-processed range-square corrected signal (RCS) in netcdf format generated by the ELPP module from the raw netcdf files submitted by each station. These products were generated in a full automatic way and in real time. At the same time the ELPP outputs were stored, an email was automatically sent to the contact point of the originating station. This email gave a real time feedback from the SCC about the pre-processing status and revealed to be extremely useful for real time fine-tuning the SCC configuration of each individual system and of its associated products.

- SCC-2: optical processed files generated by ELDA from SCC-1 products. These products are netcdf files containing the profiles of the aerosol optical coefficients: backscatter in daytime (using SCC system configurations defined for daytime condition for each lidar) and backscatter and extinction in nighttime (using SCC system configurations defined for nighttime for each lidar). The lidar configuration (daytime or nighttime) to use for the SCC analysis of each raw lidar time series is selected automatically; time series containing Raman channels are assigned to nighttime configuration while elastic-only datasets are analyzed using daytime configuration.

The netcdf files generated by ELDA are of two types:

- b-files (b for backscatter) contain at least a profile of the aerosol backscatter coefficient ($m^{-1}\,sr^{-1}$) derived from the elastic backscatter signal. This backscatter

AMTD
8, 6599–6659, 2015

EARLINET: potential operationality of a research network

M. Sicard et al.

profile may be accompanied by an extinction coefficient profile. This extinction coefficient profile is not necessarily derived from Raman measurements. Any other method to derive the extinction profile may be used here.

- e-files (e for extinction) contain profiles of aerosol extinction coefficient (m^{-1}) and of aerosol backscatter coefficients retrieved independently from a Raman channel without a priori assumptions on the existing relationship between them. Also, extinction coefficient profiles derived from high spectral resolution lidars are included here.

Both types of files include the profile of the statistical error associated to the variables they contain. Additionally they can also include other variables such as the lidar ratio, the particle linear depolarization ratio, and the water vapor mixing ratio profiles.

As summarized in Table 2, a total of 662 files were sent to the SCC. The ELPP module was successful in pre-processing 648 of them (98 %). For a minor subset (14 files) the signal quality was not sufficient to pass ELPP quality control tests in two procedures: in applying the gluing algorithm and the dead time correction to photon-counting channels. The automatic procedure of gluing between analog and corresponding photon-counting signals consists in enhancing the detected dynamic range using the analog profile in the strong signal region and the photon-counting profile in the weak signal region. The gluing algorithm implemented in ELPP tries to find the optimal region where to combine the two signals performing a set of statistical and consistency tests (D'Amico et al., 2015b) to assure a reliable and stable combined signal. When such a region was not found ELPP stopped the analysis and returned a specific error code. This is illustrated in the left panel of Fig. 2. On a total of 14 cases for which the raw data quality was not sufficient to pass ELPP quality control tests, 7 are the results of the gluing procedure, 6 refers to a problem in applying dead time correction to photon-counting channel and finally in 1 case there are format problems in the submitted raw netcdf file.

AMTD
8, 6599–6659, 2015

The number of SCC-2 profiles is 555, which represents 84 % of all submitted files (86 % of the files that passed ELPP). This percentage is quite large taking into account that no cloud screening was performed on lidar data. If we remove from the statistics the number of measurements identified a posteriori as contaminated by clouds (see next paragraph), this percentage increases up to 90 % (92 % of the files that passed ELPP). Most of the remaining 10 % (8 % with respect to the files that passed ELPP) that were not successfully inverted by ELDA were due to low signal to noise ratio in at least one of the channel of the system. Even though the same number of stations run systems equipped with channels at 355 nm than visible ones (8 stations, see Table 1 ignoring PA), the number of b-files at 355 nm (440) is lower than at 532 nm (452). This can be explained considering that the shorter is the wavelength the weaker is the contrast between aerosol and molecular contribution in lidar signals. As a consequence, in general, the retrieval of the aerosol backscatter coefficient is more problematic in the UV than in the visible or in the infrared spectral regions.

The reasons for which ELDA could not perform successfully the optical processing of SCC-1 data is shown in the right panel of Fig. 2. There are a total of 93 cases. Almost all of them (90 cases, i.e. 97 % of them) refer to the automatic search in finding a reliable and stable region for the calibration of aerosol backscatter coefficient. This search is unsuccessful typically when the pre-processed lidar signals are characterized by a poor signal-to-noise ratio (SNR) or when there is cloud contamination in the lidar profiles. To calculate the calibration factor, ELDA calculates a mean value and standard deviation in a calibration window. If that standard deviation is lower than a pre-defined maximum allowable threshold, the mean value is used to calibrate the profile. If it is larger, ELDA tries to find another calibration window within the predefined altitude region (mostly covering the total free troposphere). However, depending on the aerosol loading and vertical distribution (typically high aerosol loading at low altitude resulting in a poor SNR at high altitude or aerosols present up to high altitudes), sometimes no calibration window with sufficiently low standard deviation can be identified within the free troposphere. In those cases ELDA returns the error code “No valid data points for

AMTD
8, 6599–6659, 2015

calibration”. In particular it has been verified on the SCC-1 products that 44 (out of 90) cases for which ELDA could not find a calibration interval with the required accuracy contained clouds. The rest of the cases (46) were due mostly to problems in inverting the UV wavelengths (351 and 355 nm, 43 cases) and only occasionally 1064 nm (3 cases). The inversion at 532 nm was always successful. Among those 46 cases, the imposibility of finding a calibration interval occured twice more during daytime when applying the elastic algorithm (31 cases) than during nighttime when applying the Raman algorithm (15 cases). All 46 cases occurred at five stations (BA: 13, CL: 1; LA: 10, PO: 9, AT: 13) which means that the SCC inversion was always successful at the other five stations (leaving apart the cloud cases). This is probably due to a generally better SNR at those stations or due to different atmospheric conditions. Finally, in only one case ELDA could not find a solution for the calculation of the elastic backscatter profile with the iterative method due to a not converging iterative procedure. Such kind of situation is common (especially for shorter wavelengths) when there is a strong contamination of clouds in the lidar signals. It has been verified a posteriori that the profile contained clouds.

The SCC works as an online tool: regularly new SCC versions including debugging and improvements are provided. When a new version is set up, the whole dataset is inverted again automatically, so that the number of retrieved profiles may change, and hopefully increase. Currently the cloud screening is under development as a separate tool and different approaches to perform a reliable and robust cloud screening at network level are in testing phase. Once implemented in the SCC, it will identify cloudy conditions before the analysis which will allow us to gain computing time but not to increase the number of successful inversions.

3 The 9–12 July 2012 measurement exercise

During the time window for the “GO” (2–12 July 2012) no strong levels of PM_{10} were predicted around the Mediterranean Basin. On 3 July a weak intrusion of Saharan

AMTD
8, 6599–6659, 2015

dust was predicted to start on 5 July. The dust would come from the Libyan coasts towards south Italy and then would move eastward. Maxima of dust concentration were expected on 6–7 July. The forecast on 4 July confirmed the intrusion of 5 July with two important changes: Spain would also be affected by the intrusion and the event would strengthen starting on 8 July. The "GO" was fixed to Monday 9 July at 06:00 UT. The exercise ended on Thursday 12 July at 06:00 UT. The days of interest, 9, 10, 11 and 12 July, are hereinafter noted as J09, J10, J11 and J12, respectively.

3.1 Synoptic situation

Figure 3 shows the synoptic situation centered over the Mediterranean Basin in terms of sea level pressure for the three periods 00–24, 24–48 and 48–72 h after the "GO". Each map is a composite map from the NCEP/NCAR (National Centers for Environmental Prediction/National Center for Atmospheric Research) Reanalysis project showing the mean sea level pressure for each period. The period is characterized by the presence of a stable Azores high and three low pressure systems centered over southern Norway, Saudi Arabia and Mali. A warm front associated with the low pressure system located over southern Norway produced unstable weather over northern Europe and high temperatures and fair weather over western and central Europe. This situation generated generally clear skies above the northern part of the Mediterranean Basin, the region of interest, which persisted during the period as the Azores High moved slightly eastward. Easterly winds were also predominant over Europe.

The Saharan dust intrusion forecasted to start on 5 July occurred indeed. It was a rather moderate event that did not affect all the stations involved in the 9–12 July measurement exercise as forecasted by dust transport models. The AERUS-GEO daily aerosol optical depth at 675 nm on J09, J10, J11 and J12 from the MSG/SEVIRI sensor is shown in Fig. 4. Figure 4 shows how the dust, transported above northern Morocco, Algeria and Tunisia, hits the southeastern coasts of Spain as well as southern Italy, disperses above the western Mediterranean Basin and moves slowly eastwards. It also shows the intensity decrease of the dust event from J09 until J12. It is not clear if the

AMTD
8, 6599–6659, 2015

dust plume reaches Greece and Romania. According to Fig. 4 the only stations that are very likely to have been hit by the event are Granada and Potenza. The maximum dust concentration forecast by the BSC-DREAM8b model was ~ 170–180 $\mu g\,m^{-3}$ over L'Aquila and Potenza on J09 at 12:00 UT and over Granada on J12 at 12:00 UT (after the exercise ended).

In addition to mineral dust, fires are also frequent around the Mediterranean Basin at this period of the year. The fire overlays from the MODIS sensor onboard Aqua and Terra satellites are shown in Fig. 5. Many fires are present on the northern coast of Algeria, in Sicily and in southern Italy. The fire smoke could be mixed with the dust plume which is visible on MODIS images. A series of fires are also present from west to east between the countries of the ex-Yugoslavia and southern Romania.

3.2 Spatial and temporal (4-D) evolution of the atmospheric aerosols

In this section, all the SCC-1 and SCC-2 products, but not only, are shown in order to characterize spatially and temporally the aerosol loading around the Mediterranean Basin during the period J09–J12. This section aims at illustrating the range of SCC products that EARLINET is able to provide in real and near-real time under some given circumstances. A more comprehensive analysis of the dust microphysics during the operationality exercise can be found in Granados-Muñoz et al. (2015). To get a general overview of the situation we first plot in Fig. 6 the sun-photometer AOD at 532 nm calculated from the measured AOD at 440 nm, and the Ångström exponent (AE) calculated between the wavelengths at 440 and at 675 nm. Only level 2.0 data (cloud screened and quality assured) were used. Clermont-Ferrand and Potenza are not shown in Fig. 6. In Clermont-Ferrand the AERONET data are very sparse because of the presence of broken clouds. No AERONET data are available at Potenza during the exercise because the instrument was back to NASA Goddard for calibration. A striking feature is that, except at Granada, the AE is larger than 1 at all stations. In Bucharest and Limassol it is often closer to 2 than to 1. This is an indication that mineral dust may not have been detected at those stations. At

AMTD
8, 6599–6659, 2015

Granada, the AE is below 0.5 on J09 which suggests that dust was present. On J10 and J11 the AOD is moderate (< 0.2) and the AE seems to increase to values comprised mostly between 0.5 and 1. Dust might still be present on both days in Granada.

Time-height series of the semi-attenuated backscatter coefficient (not a SCC product). Time-height series, also called quicklooks, of the attenuated backscatter coefficient not corrected for the total transmissivity are shown in Fig. 7 for Évora, Barcelona and Bucharest at 1064 nm. The attenuated backscatter not corrected for the total transmissivity was calculated by fitting the RCS to the molecular slope in an aerosol-free region. To do so, the RCS, $P(z)$, at altitude z was fitted to the profile of the molecular backscatter coefficient, $\beta_m(z)$, in an aerosol-free region centered around a reference altitude, z_{ref}. The attenuated backscatter not corrected for the total transmissivity, $\beta_{att\text{-}uncorr}$, and the attenuated backscatter, β_{att}, are related through:

$$\beta_{att\text{-}uncorr}(z) = \frac{\beta_T(z)T_T^2(z)}{T_T^2(z_{ref})} = \frac{\beta_{att}(z)}{T_T^2(z_{ref})}, \quad (1)$$

where β_T and T_T refer to the total backscatter coefficient and the total transmissivity, respectively. The thickness of the fitting region was fixed to 1 km around the reference altitude which was selected within the range 5.5–7.5 km depending on the aerosol stratification. Quicklooks are not a standard product of the SCC but their representation gives an excellent overview of the aerosol load vertical distribution and temporal evolution at each station.

Three very different situations are observed. In Évora almost no clouds are observed during the whole event. The diurnal evolution of the AOD (Fig. 6) is correlated with that of $\beta_{att\text{-}uncorr}$ in the planetary boundary layer (PBL). Hardly any lofted layers are observed above the PBL. The maximum values of the AOD, approximately 0.1, reached between 12:00–15:00 UT coincide with minimum values of the AE. Those results indicate that Évora was only influenced by local aerosols.

AMTD
8, 6599–6659, 2015

In Barcelona $\beta_{\text{att-uncorr}}$ is quite strong in the first kilometer where the PBL top is usually detected (Sicard et al., 2011). The AOD which oscillated around 0.2 comes to be a seasonal value (Sicard et al., 2011). In the quicklook, many layers of different intensities are observed in the troposphere and up to 5 km. In the afternoon of J10 the sun-photometer AOD decrease is associated with an increase of the AE and with an apparently thinner lofted layer coming down from ~ 4 to ~ 2 km.

The aerosol stratification in Bucharest is also complex. The PBL formation is clearly visible every morning after 06:00–07:00 UT. At all times, aerosol layers are observed in the troposphere and up to 6 km. Every day the AOD ranges between 0.2 and 0.5 while the AE ranges between 1.5 and 2.0. Two phenomena are observed in terms of AOD and quicklook of attenuated backscatter not corrected for the total transmissivity: (1) in the afternoon of J10 the AOD increase coincides with the arrival of a layer between 2 and 5–6 km, and (2) the sharp AOD decrease on J11 coincides with the sinking of the lofted layer.

RCS profiles at several wavelengths (SCC-1 products).

The products from ELPP, i.e. the RCS profiles at 355 and 532 nm, on J11 are shown in Fig. 8 for the same stations as in Fig. 7. The RCS units are arbitrary units. The *x* axis limit of Fig. 8 has been optimized to highlight the layers with aerosols. The regions where the RCS profiles exceed the selected *x* axis limit are usually contaminated by clouds. At all three stations no overlap correction was performed, thus the first hundreds of meters above the lidar stations are clearly affected by the incomplete overlap effect and are not representative of the aerosol load. The time series of the hourly RCS profiles show clearly the periods contaminated by clouds: between 05:00 and 08:00 UT in Évora, between 02:00 and 05:00 UT and between 07:00 and 11:00 UT in Barcelona, and at 02:00, 04:00, 05:00 and 07:00 UT in Bucharest. The features commented in the former paragraph about the quicklooks, such as the diurnal cycle of the PBL in Évora or the sinking of the lofted layers in Bucharest between 06:00 and 12:00 UT, are also visible here. We recall that ELPP generates an intermediate product that is not easily usable for direct science purposes but that is extremely useful for validation of and/or assimilation in air quality and climate models (see Sect. 4).

Backscatter coefficient profiles at several wavelengths (SCC-2 products).

The ELDA module of the SCC provides inversions of the aerosol optical properties. During daytime all elastic wavelengths are inverted by means of the elastic algorithm (see Mattis et al., 2015). Figures 9 and 10 show the temporal evolution of the profiles of the backscatter coefficient at all stations with at least two wavelengths on J10. Figure 9 reports the results at the Iberian stations and Fig. 10 at the central and eastern European stations. All the profiles are reported as a function of height above mean sea level. This is the reason why the different stations present profiles starting at different heights in agreement with their respective altitudes above sea level. Some inversions are missing in the middle of the day at Barcelona, Potenza, Bucharest and Limassol. In Barcelona, the lidar system had a misalignment problem in the optical channel at 355 nm which resulted in a very poor SNR at 355 nm that has prevented ELDA to find a calibration interval with the required accuracy during daytime. In Potenza, in 8 cases, among which 2 of them were identified a posteriori as contaminated by clouds, ELDA could not find a calibration interval. In Bucharest, the missing inversions were due mostly to the search in finding a reliable region for the aerosol backscatter calibration and also to the not converging iterative procedure. We verified a posteriori that all missing inversions in Bucharest contained clouds that can be actually seen in Fig. 7c. In Limassol no measurements were performed between 09:00 and 14:00 UT on J10 because of technical problems with the laser transmitter. It is worth noting that the SCC is configured so that it returns the full set of products of a defined system configuration only if the inversion of all products is performed successfully (pre-processing and optical processing). If a single product is not retrieved successfully, no inversion at all is delivered. It is a way to guarantee a high quality of all the products defined in a system configuration and delivered by the SCC. The drawback is that if the quality of the raw data is not sufficient for the analysis, the raw data do not pass the quality control tests of the analysis algorithms and the SCC does not return any result for the corresponding measurement. During nighttime the SNR is higher than during daytime and the inversion (mostly at 355 or at 532 nm) is statistically more successful during nighttime than during daytime, especially around the hours when the sun is close to zenith (Mattis et al., 2015).

Except near the surface where none of the systems is corrected for the incomplete overlap and for obvious cloudy cases, the backscatter coefficient in general does not exceed 3 $\mathrm{Mm^{-1}\,sr^{-1}}$. In Athens the backscatter coefficient at 355 nm is higher, reaching regularly 4 $\mathrm{Mm^{-1}\,sr^{-1}}$ in the tropospheric layers. Except in Évora where the troposphere is particularly clean during the whole period, tropospheric aerosols are present in general between 2 and 5 km and sometimes up to 6 km (in Potenza). In Granada the aerosol layer above 2–3 km has a very low spectral dependency (especially visible between the profiles at 355 and 532 nm) which indicates the presence of mineral dust. This low spectral dependency is also observed on the profiles of Potenza above 4 km in the early hours of J10, which also confirms the presence of mineral dust but at a higher altitude compared to Granada.

Extinction coefficient profiles at several wavelengths (SCC-2 products).

During nighttime the Raman algorithm allows for the retrieval of the extinction coefficient in addition to the backscatter coefficient. The profiles of the extinction coefficient at 355 and at 532 nm are shown in Fig. 11 at two stations of the Iberian Peninsula (Granada and Barcelona on the night J09–J10) and at 2 stations of central and eastern Europe (Potenza and Bucharest on the night J10–J11). The plots at Potenza and Bucharest are shown 24 h after the selected night at Granada and Barcelona in order to maximize the probability of presence of mineral dust in the profiles (see Fig. 4). As it can be seen in Fig. 11, the temporal continuity of the retrieved profiles reveals the correct functioning of the SCC in nighttime conditions.

All extinction profiles stay in general below 400 $\mathrm{Mm^{-1}}$. Low spectral dependency between both profiles at 355 and at 532 nm is observed at Granada above 2 km

AMTD
8, 6599–6659, 2015

EARLINET: potential operationality of a research network

M. Sicard et al.

and at Potenza in the whole profile, and indicates the presence of mineral dust at both stations. In Barcelona the profiles at both wavelengths are quite different and suggest different signal levels: the large oscillations at 355 nm reflect lower SNR compared to 532 nm. In Bucharest the extinction coefficient is almost twice larger at 355 nm than at 532 nm, which is consistent with the high AE found on the AERONET data (Fig. 6). An aerosol layer is clearly visible until 2 km and another one up to 5–6 km, reaching peak values at heights between 3 and 4 km. Those vertical profiles of optical properties are in agreement with the microphysical retrievals presented in Granados-Muñoz et al. (2015) who found a strong contribution of non-spherical coarse particles in the lofted layers on J09 in Granada, and a strong contribution of fine particles in the lofted layers on J11 in Bucharest.

Parameters derived from the SCC-2 products.

The Raman and the multi-wavelength capabilities of the advanced systems allow for the retrieval of derived products such as:

– The backscatter-related AE between the wavelengths (355, 532 nm; $AE_{355–532}$), (532, 1064 nm; $AE_{532–1064}$) and (355, 1064 nm; $AE_{355–1064}$).

– The extinction-related AE between the wavelengths (355, 532 nm).

– The lidar ratios (LR), the extinction-to-backscatter ratio, at 355 (LR_{355}) and at 532 nm (LR_{532}).

– The color ratios, the ratio of the backscatter coefficients, between the wavelengths (355, 532 nm; $CR_{355–532}$), (532, 1064 nm; $CR_{532–1064}$) and (355, 1064 nm; $CR_{355–1064}$).

The color ratios and the backscatter-related AE have the same physical meaning, thus the color ratios are listed here and presented in Fig. 12 only for completeness and are not discussed in the text. It is worth noting that those four derived products

AMTD
8, 6599–6659, 2015

are all intensive aerosol parameters that are extremely valuable for aerosol classification (Müller et al., 2007b; Burton et al., 2012; Groß et al., 2013). Figure 12 shows all nighttime direct and derived SCC-2 products at the same stations than in Fig. 11 and for a selected time during the night J09–J10 at the Iberian stations and during J10–J11 at the other two stations. The SCC-2 products were not manipulated so that at high altitude in aerosol-free regions some products (AE, LR and CR) stop from having a physical meaning. By plotting backscatter and extinction coefficients side by side, the overlap effect present in the first hundreds of meters of the extinction coefficient profile (and not on the backscatter coefficient profile) is shown. We recall that for that reason the first hundreds of meters above the lidar stations of the profiles of the extinction coefficient and the products derived from them are not representative of the aerosol load. In the plots of the extinction coefficient profiles we also report the integral of the extinction profiles at both wavelengths of 355 and 532 nm. Even though those values should be a little lower than the AERONET AOD since no extinction values are provided in the first hundreds of meters, the comparison with the AERONET AOD gives an indication on the contribution of the tropospheric layers to the total AOD. In order to have an idea of the origins of the air masses at each site, 4 day backtrajectories were calculated at three heights within the observed aerosol layers with the Hybrid Single Particle Lagrangian Integrated Trajectory (HYSPLIT) model (Draxler and Rolph, 2003; Rolph, 2003) provided by the NOAA-ARL (National Oceanic and Atmospheric Administration – Air Resources Laboratory). They are shown in Fig. 13. At last, the backscatter and extinction coefficients retrieved by the SCC were compared to the manual inversions provided by each group. It is worth noting that D'Amico et al. (2015b) show that there is no climatological bias between SCC and manual retrievals.

In Granada two layers are detected: one below 2 km and another one above up to 4–4.5 km. The integral of the extinction coefficient profiles (0.22 and 0.27 at 355 and 532 nm, respectively) are in agreement with the last AERONET AOD at 532 nm measured on J09 which varies between 0.2 and 0.3 at 532 nm (Fig. 6). All SCC profiles have been compared to the manual inversions provided by the Granada group (not

AMTD
8, 6599–6659, 2015
EARLINET: potential operationality of a research network
M. Sicard et al.

shown) and one difference appears: the SCC profile of the backscatter coefficient at 1064 nm is lower (by a roughly constant value of −1.2 to −1.0 $Mm^{-1} sr^{-1}$) with respect to the manual inversions. This discrepancy is mainly due to different approaches used to calibrate the elastic backscatter at 1064 nm. The SCC calibration is made following the procedure provided by Mattis at al. (2015) constraining, within the calibration range, the aerosol backscatter coefficient to a fixed climatological value. On the other hand, the calibration of the manually inverted backscatter coefficient at 1064 nm is made according to Engelmann et al. (2015). In particular the information available at other wavelengths (355, and 532 nm in this case) is used to constrain the aerosol backscatter reference at 1064 nm. This approach cannot be used by the SCC because, in the current version, it does not implement retrieval procedures combining aerosol products calculated at different wavelengths. In the framework of the upcoming ACTRIS-2 project, EARLINET is working to implement in the SCC such kind of advanced analysis procedures and also to set-up a multi-wavelength post-retrieval quality check for both manual and SCC inversions. Above 2 km the extinction coefficient profiles at 355 and at 532 nm overlap, which results in an extinction-related AE close to 0. This low value of the extinction-related AE indicates the presence of large particles such as mineral dust. The backtrajectories at 2.5 and 4 km are originating along the coasts of Morocco where dust is detected on the MSG/SEVIRI AOD maps (Fig. 4). The backtrajectories arriving in Granada at 1500 m seems to have a north Atlantic origin. Except for a peak at 80 sr, LR_{355} varies between 55 and 70 sr while LR_{532} varies between 45 and 65 sr between 2 and 4 km. The values found for the lidar ratios and the extinction-related AE are in agreement with previous observations of Saharan dust in Granada (Guerrero-Rascado et al., 2008, 2009; Córdoba-Jabonero et al., 2011).

In Barcelona several layers are observed up to ∼ 4.5 km. The integral of the extinction coefficient at 532 nm, 0.06, is rather low compared to the AERONET AOD in the early hours of J10 (> 0.2, Fig. 6) which suggests that either most of the AOD is confined in the lowermost layer (< 1 km) or that the aerosol load has changed. The agreement between SCC and manual retrievals is good, even though larger variations,

Discussion Paper | Discussion Paper | Discussion Paper | Discussion Paper |

AMTD
8, 6599–6659, 2015

EARLINET: potential operationality of a research network

M. Sicard et al.

probably due to different vertical resolutions, are observed on the manual retrievals. The backscatter-related AE are quite variable from one pair of wavelengths to another while the extinction-related AE is often larger than 2, a value quite larger than the mean summer value of 0.82 given by Sicard et al. (2011). LR_{532} reaches values in the range 15–30 sr. An a posteriori verification on the SCC-1 profiles reveals a small contamination of clouds in the layer centered at 1.5 km. The backtrajectories shown in Fig. 13b indicate that the air masses arriving in Barcelona at 1.5 km have a local origin (re-circulation patterns) while those arriving at 2.5 and 4 km have a clear origin over the Atlantic Ocean. In spite of the large variability of the aerosol intensive parameters derived from the SCC-2 products, the results obtained (large extinction-related AE and low LR_{532}) together with the backtrajectories indicate that marine aerosols are likely present.

From the backscatter coefficient profiles in Potenza, three aerosol layers stand out: one up to 1.7 km, a second one between 1.7 and 2.5 km and another one between 2.5 and 3.5 km. The agreement between the manual inversions provided by the Potenza group (not shown) and the SCC profiles is very good. Only one significant discrepancy, which might also be due to different vertical resolutions, is observed on the extinction coefficient at 532 nm in the range 1.7–2.5 km which is in average around 15 Mm^{-1} for the SCC and 35 Mm^{-1} for the manual inversion. One observes that the higher the aerosol layer, the lower the spectral dependency. This behavior is well reproduced on the backscatter-related AE that decrease with increasing height and that are similar and lower than 1 at almost all heights. In the uppermost layer (2.5–3.5 km) all AEs are lesser than 0.5. The lidar ratios in the same interval range are similar and vary between 40 and 55 sr. Those results (low AE; $40 < LR < 55$ sr) reveal the presence of mineral dust in the aerosol layer between 2.5 and 3.5 km, a conclusion that is confirmed by the backtrajectories arriving in Potenza at 3 km (Fig. 13c) which are originating along the coasts of Morocco where dust is present (see the MSG/SEVIRI AOD maps in Fig. 4). These results are in agreement with previous studies on Saharan dust observations over Potenza by Mona et al. (2006, 2014). Over about 6 years of Raman measurements

AMTD
8, 6599–6659, 2015

LR_{532} for dust (pure and mixed situations) is found to be in the range 40–70 sr and is typically increasing with decreasing AE (Mona et al., 2014).

In Bucharest two main layers are visible on the backscatter coefficient profiles: one between 1.0 and 2.5 km and another one centered around 4 km. The integral of the extinction coefficient profile at 532 nm (0.18) is in agreement with the AERONET AOD (∼ 0.3 at 532 nm in the late afternoon of J10) if we assume that the extinction coefficient in the bottom layer (not retrieved in the plot) contributes significantly to the total AOD. The agreement between SCC and manual retrievals is very good. No significant differences are observed. A clear spectral dependency arises from the optical coefficients resulting in Ångström exponents relatively high. The lidar ratios are slightly different between one layer and the other: $LR_{355} \sim 30$ sr and $LR_{532} \sim 40$ sr in the range interval 2–3 km while $LR_{355} \sim 45$ sr and $LR_{532} \sim 38$ sr in the layer centered around 4 km. All three backtrajectories arriving in Bucharest at 1.5, 2.5 and 4 km come from the same direction: west-southwest. According to Burton el al. (2012) the combination of $AE_{532-1064} \sim 1.1$ (which represents a color ratio 532/1064 nm near 2) and $LR_{532} \sim 40$ sr (at 2–3 km) and around 38 sr (in the layer centered around 4 km) could indicate urban aerosols and/or smoke at 2–3 km and fresh smoke in the uppermost layer. MODIS fire maps (Fig. 5) on J09 and J10 indicate the presence of fires in southern France and in the northern Balkan countries. Our results are in agreement with observations of fresh and aged biomass burning in Bucharest (Nicolae et al., 2013), in which fresh and aged smoke particles are distinguished by means of their Ångström exponents and the ratio of their lidar ratios (LR_{532}/LR_{355}). Also Granados-Muñoz et al. (2015) found that the aerosol size distribution in Bucharest was dominated by small particles, especially on J11.

4 Potential operationality of EARLINET

The EARLINET 72 h measurement exercise performed in July 2012 demonstrates the potential operationality of an aerosol lidar research network formed mostly by advanced lidar systems. SCC-1 and SCC-2 products for this field campaign have been processed and are available to the scientific community on request. More details about the EARLINET data policy can be found in the EARLINET website (http://www.earlinet.org/).

Even if the exercise duration is rather short, it demonstrates that all techniques, infrastructures, and procedures are ready for the operationality of the network. The only limiting factor is the cost of operation. In that line, the automation or semi-automation of many EARLINET advanced lidar systems is ongoing in order to decrease drastically the cost of operation. The data from the EARLINET 72 h measurement exercise, SCC-1 products in this case, partly or as a whole, are also used by the EARLINET community itself for investigating new retrieval methods (Bravo-Aranda et al., 2014; Banks et al., 2014) and evaluating different PBL schemes in the Weather Research and Forecasting (WRF) model (Banks et al., 2015). The results from the exercise allow to tackle many fields related to atmospheric aerosols: monitoring of special events (Saharan dust intrusions, spread of volcanic ash plumes, transport of biomass burning or export of contamination), atmospheric modelling (air quality models, dust transport models, numerical dispersion and weather models), climate research (model evaluation at the scale of the event, aerosol transport and tracers, impact on radiation) and calibration/validation activities of spaceborne lidars.

Monitoring of special events.

The specific observations performed by EARLINET during special events such as Saharan dust outbreaks, volcanic eruptions and biomass burning (see references in the introduction) are not continuous measurements. Even if today those measurements can be processed by the SCC in near real time fulfilling simultaneously the quality standards of EARLINET (D'Amico et al., 2015a, b), their temporal discontinuity and heterogeneity would make the spatio-temporal monitoring of a special event difficult. By applying the measurement protocol defined in Sect. 2.2, EARLINET is able to perform continuous measurements in order to provide real time SCC-1 products. This capability has a tremendous outcome for what concerns continental scale volcanic eruptions such

AMTD
8, 6599–6659, 2015

as the one of the Eyjafjalla volcano in 2010 (Ansmann et al., 2010; Groß et al., 2011; Sicard et al., 2012; Pappalardo et al., 2013, among others). Such events, which represent a hazard for a large number of human activities, could be monitored firstly in real time (SCC-1 products) for their spatio-temporal distribution and secondly in near-real time (SCC-2 products) for quantifying the aerosol optical properties and concentration.

Atmospheric modelling.

In the field of atmospheric modeling real time SCC-1 and near-real time SCC-2 products are also of great interest, in particular for air quality, dust transport, and numerical dispersion and weather forecasts.

Recent air quality modelling studies have shown that the assimilation of ground-based PM_{10} measurements by a mesoscale chemical-transport model only constrains the model over a few hours and does not improve the forecast over time scales larger than 24 h (Tombette et al., 2009). In situ surface measurements do also not provide information on the vertical profiles. Although the persistence of forecast improvement of PM_{10} is short when ground-based PM_{10} measurements are assimilated, the assimilation of lidar measurements is expected to lengthen the time scale over which the forecast may be improved, by adding information on the vertical concentration of particles and constraining the transport. Indeed the EARLINET 72 h measurement exercise already led to significant results in that field: Wang et al. (2014) assimilated the SCC-1 products in the Eulerian chemistry transport model POLAIR3D (Sartelet et al., 2007) of the air quality platform POLYPHEMUS (Mallet et al., 2007). Their findings indicate that a horizontal correlation length of 100 km, an assimilation altitude range of 1–3.5 km and an assimilation period length of 12 h give the best scores for PM_{10} and $PM_{2.5}$. Additionally, the authors find that the temporal impact of assimilating lidar signals is longer than 36 h after the assimilation period. The advantage of using SCC-1 products is that they are generated with a higher success rate than SCC-2 products. For example, in the present exercise, 98 % (against 75 %) of all submitted file provided SCC-1 (SCC-2) products.

AMTD
8, 6599–6659, 2015

Saharan dust is an important contributor on European air quality levels and consequently has a relevant impact on human health and ecosystems. Even though most of the transport of dust particles occurs in altitude, dust events impact surface PM_{10} concentrations (Pey et al., 2013), hence the need to model properly their vertical and horizontal transport. Regional dust models need to be evaluated against observations to identify their strengths and weaknesses in reproducing the quantitative and qualitative dust layer properties. The first systematic comparison of modeled dust extinction profiles vs. Raman lidar measurements has been recently published using the BSC-DREAM8b model, one of the most widely used dust regional models in the Mediterranean, and Potenza EARLINET lidar profiles for Saharan dust cases (Mona et al., 2014). More recently Granados-Muñoz et al. (2015) uses the EARLINET 72 h measurement exercise to compare locally in Granada several dust transport models with the observations. At a larger scale, Papayannis et al. (2008) and Binietoglou et al. (2015) report the comparison of one and four dust transport models, respectively, with EARLINET observations. The evaluation of aerosol models like the SEEVCCC (South East European Virtual Climate Change Center) DREAM model and the EMEP/MSC-W (EMEP/Meteorological Synthesizing Centre – West) model, with aerosol profiles measured during the whole summer 2012 ACTRIS campaign is currently ongoing (Vukovic et al., 2104; Tsyro et al., 2014). At the regional scale, the EARLINET 72 h measurement exercise represents a great potential for real time monitoring, estimation and validation of regional dust models since it provides on a regional scale the structural and optical properties of the dust layers during a continuous period of time. The real time requirement is an important issue since for the evaluation of operational dust models SCC-2 products are needed. The potential operationality of EARLINET, but not only, is also fundamental for the reliability of mineral dust forecasting and early warning system such as the WMO Sand and Dust Storm Warning Advisory and Assessment System (SDS-WAS) which usually rely on the output of several models (see http://sds-was.aemet.es/).

AMTD
8, 6599–6659, 2015

The use of aerosol data for assimilation in a numerical weather prediction model is very recent: Collins et al. (2001) and Rasch et al. (2001) focused on regional studies while Benedetti et al. (2009) assimilated aerosol data globally. At the global scale, the first attempt was made with aerosol optical depth from satellite sensors. Again, like in air quality modelling, the information on the vertical distribution of the aerosols is not taken into account. As far as we know, aerosol lidar data have never been assimilated in a weather prediction model, the main reason being that the development of aerosol modules for weather prediction model is relatively new. So there is a large community that will be interested, likely in the near future, in using aerosol lidar data for assimilation in weather prediction models. The EARLINET 72 h measurement exercise is a great opportunity for weather modelers to investigate the feasibility of lidar data assimilation in weather forecast modelling at the regional scale in a first approach. For the assimilation to be efficient, a lot of research remains to be done in that field, in particular on the coupling of the aerosol module with the meteorology and in general on the aerosol interactions with the atmospheric system as a whole. Related to weather prediction models and special event monitoring, mass densities derived from SCC-2 products during a special event can help to improve the first guess estimates of the aerosol (typically ash, smoke or dust) emissions which are required as input for numerical dispersion models.

Climate research.

In climate research continuous lidar measurements are of interest for the validation of regional climate modelling at the scale of the event. Once those models have shown their ability to simulate the evolution of aerosols during a given event (e.g., in terms of spatial pattern, daily variability, plume vertical distribution, particle size distribution, etc.), they are usually used to study the impact of dust outbreaks on regional climate (Nabat et al., 2015). The EARLINET 72 h measurement exercise represents an ideal tool for the validation of such models since it provides hourly extinction coefficient pro-

AMTD
8, 6599–6659, 2015
EARLINET: potential operationality of a research network
M. Sicard et al.

files (SCC-2 profiles) at several sites around the Mediterranean basin. Real time is not a requirement for such kind of validation.

When radiation flux measurements are not available, SCC-2 products can be used to calculate locally the aerosol direct radiative forcing (ADRF) with 1-D radiative transfer models. Continuous measurements offer the possibility to compare on an hourly basis the shortwave and longwave component and quantify the compensation of the shortwave by the longwave, especially during nighttime. In turn those local estimations of the ADRF can be used to constrain regional climate model.

Calibration/validation activities of spaceborne lidars.

The validation of ongoing and the preparation of future satellite-based lidars has been a continuously ongoing activity of EARLINET that started before the launch in 2006 of the Cloud Aerosol Lidar and Infrared Pathfinder Satellite Observations (CALIPSO) mission. At network level, a measurement plan was developed and optimized. The coordinated efforts permitted to validate at continental scale different CALIPSO products and to foster new improvements in CALIPSO data (e.g. Pappalardo et al., 2010; Wandinger et al., 2011). Collected measurements (The EARLINET publishing group 2000–2010, 2014) were the pillar for investigating the effects of local variability on validation studies (e.g. Mamouri et al., 2009; Mona et al., 2009). Nowadays EARLINET activities in satellite data validation have increased: investigation of climatological CALIPSO products, and participation in design and optimization of lidar measurements for next to come lidar-based satellite missions like ADM-Aeolus (Atmospheric Dynamics Mission) and EarthCARE (Earth Clouds, Aerosols and Radiation Explorer). Moreover within the Copernicus programme, other sensors will be launched in space for aerosol monitoring at global and continental scale. EARLINET is already committed by the European Space Agency (ESA) for the validation of ADM-Aeolus and Copernicus Sentinel-5 Precursor missions. All those activities will require important efforts for performing measurements, analyzing them and using them for validation studies. The use of the SCC would represent a valuable help for calibration/validation

AMTD
8, 6599–6659, 2015

activities of spaceborne lidars by reducing the efforts of data manipulation. In addition, there is an always increasing request for near-real time validation for which SCC is particularly important as this study demonstrates.

5 Conclusions

In the framework of ACTRIS summer 2012 measurement campaign (8 June–17 July 2012), EARLINET organized and performed a controlled exercise of feasibility to demonstrate its potential to perform operational, coordinated measurements. Eleven lidar stations distributed on the northern Mediterranean Basin participated to the exercise which started on 9 July 2012 at 06:00 UT and ended 72 h later on 12 July at 06:00 UT. This time period was selected in order to track at the regional scale a Saharan dust intrusion forecasted originally to hit first Spain and move eastward during the period of the exercise. The measurements had to be provided at all the wavelengths available at each station and at the system raw temporal and spatial resolutions. No cloud screening had to be applied. At the end of each measurement all stations were required to send their measurements in real time in a predefined netcdf file format to a centralized server.

For the first time the single-calculus chain developed within EARLINET was used in real time for a multitude of different systems: the pre-processing of the data (ELPP module, SCC-1 products) was performed in real time while the optical processing (ELDA module, SCC-2 products) was performed in near-real time. ELPP was configured in such a way that at the same time that the outputs were stored, an email was automatically sent to the contact point of the originating station. This email gave a real time feedback from the SCC about the pre-processing status and revealed to be extremely useful for real time fine-tuning the SCC configuration of each individual system and of its associated products. A total of 662 files were sent to the SCC. Out of them the ELPP module pre-processed successfully 648 files (98 %) while the ELDA module processed successfully 555 files (84 %). This percentage is quite large taking into account

AMTD
8, 6599–6659, 2015

that no cloud screening was performed on the lidar data. After an a posteriori manual cloud screening this percentage rises to 90 %. At the pre-processing level, the raw data quality was not sufficient to pass ELPP quality control tests in two procedures: in applying the gluing algorithm and the dead time correction to photon-counting channels. In almost all cases (97 %) for which ELDA could not derive a solution, no calibration interval could be found within the required uncertainties because either the delivered raw signals had a too low SNR or they were contamined by clouds. For the cases without cloud contamination, more succesfull inversions can be obtained if one relaxes the required uncertainties, i.e. if one allows larger uncertainties of the backscatter profiles, or if stronger averaging and smoothing is applied (Mattis et al., 2015). The developers of ELPP are working on the development of a reliable and robust cloud screening (D'Amico et al., 2015a). At last, in the framework of the upcoming ACTRIS-2 project, EARLINET is working on the set-up of a post-retrieval quality check procedure for the SCC and manual inversions.

The large amount of coordinated observations and their standardized processing yield an unprecedented data set with many promising perspectives in the field of atmospheric research. The time series of the continuous and homogeneously obtained products of ELPP, the range-square corrected signals, are not easily usable for direct science purposes but are extremely useful for validation of and/or assimilation in air quality and climate models. The optical products retrieved by the ELDA module are valuable information in fields such as the monitoring of special events, atmospheric modelling, climate research and calibration/validation activities of spaceborne observations. Derived optical products (backscatter- and extinction-related Ångström exponents, lidar ratios and color ratios) are powerful tools for aerosol typing, especially interesting for the monitoring of special events and aerosol climatology which connects to calibration/validation activities of spaceborne observations.

The efforts made to define the measurements protocol and to configure properly the SCC makes the operationality exercise repeatable for any of the applications above mentioned. In the meantime the EARLINET community is working on three aspects

AMTD
8, 6599–6659, 2015

that would improve significantly the operationality of the network and the quality of the products delivered in real time by the SCC: at the hardware level on the capability of daytime Raman measurements and at the software level on cloud screening and on smoothing procedure of daytime data. In the framework of the upcoming ACTRIS-2 project, EARLINET will also implement in the SCC a multi-wavelength post-retrieval quality check for both manual and SCC inversions.

Acknowledgements. This work is supported by the 7th Framework Programme project Aerosols, Clouds, and Trace Gases Research Infrastructure Network (ACTRIS) (grant agreement no. 262 254). Measurements in Barcelona are supported by the Spanish Ministry of Spanish Ministry of Economy and Competitivity (project TEC2012-34575) and of Science and Innovation (projects UNPC10-4E-442, CGL2011-13580-E/CLI and CGL2011-16124-E/CLI) and FEDER funds. Research activities in Granada are supported by the Spanish Ministry of Economy and Competitiveness through the project CGL2013-45410-R and by the Andalusia Regional Government through projects P10-RNM-6299 and P12-RNM-2409. Measurements in Évora were supported by FCT (Fundação para a Ciência e a Tecnologia) through the project PTDC/GEO-MET/4222/2012 and grants SFRH/BD/47521/2008 and SFRH/BPD/81132/2011. This project has also received funding from the European Union's Seventh Framework Programme for research, technological development and demonstration under grant agreement no 289 923 – ITaRS. The authors gratefully acknowledge the NOAA Air Resources Laboratory (ARL) for the provision of the HYSPLIT transport and dispersion model and READY website (http://www.arl.noaa.gov/ready.html).

References

Alados-Arboledas, L., Müller, D., Guerrero-Rascado, J. L., Navas-Guzmán, F., Pérez-Ramírez, D., and Olmo, F. J.: Optical and microphysical properties of fresh biomass burning aerosol retrieved by Raman lidar, and star-and sun-photometry, Geophys. Res. Lett., 38, L01807, doi:10.1029/2010GL045999, 2011.

Amiridis, V., Balis, D. S., Giannakaki, E., Stohl, A., Kazadzis, S., Koukouli, M. E., and Zanis, P.: Optical characteristics of biomass burning aerosols over Southeastern Europe determined

AMTD

8, 6599–6659, 2015

from UV-Raman lidar measurements, Atmos. Chem. Phys., 9, 2431–2440, doi:10.5194/acp-9-2431-2009, 2009.

Amodeo, A., D'Amico, G., Mattis, I., and Freudenthaler, V.: Error calculation for EARLINET products in the context of quality assurance and single calculus chain, Atmos. Meas. Tech. Discuss., in preparation, 2015.

Ansmann, A., Bösenberg, J., Chaikovsky, A., Comerón, A., Eckhardt, S., Eixmann, R., Freudenthaler, V., Ginoux, P., Komguem, P., Linné, H., Ángel López Márquez, M., Matthias, V., Mattis, I., Mitev, V., Müller, D., Music, S., Nickovic, S., Pelon, J., Sauvage, L., Sobolewsky, P., Srivastava, M. K., Stohl, A., Torres, O., Vaughan, G., Wandinger, U., and Wiegner, M.: Long range transport of Saharan dust to northern Europe: the 11–16 October 2001 outbreak with EARLINET, J. Geophys. Res., 108, 4783, doi:10.1029/2003JD003757, 2003.

Ansmann, A., Tesche, M., Groß, S., Freudenthaler, V., Seifert, P., Hiebsch, A., Schmidt, J., Wandinger, U., Mattis, I., Müller, D., and Wiegner, M.: The 16 April 2010 major volcanic ash plume over central Europe: EARLINET lidar and AERONET photometer observations at Leipzig and Munich, Germany, Geophys. Res. Lett., 37, L13810, doi:10.1029/2010GL043809, 2010.

Banks, R. F., Tiana-Alsina, J., Baldasano, J. M., and Rocadenbosch, F.: Retrieval of boundary layer height from lidar using extended Kalman filter approach, classic methods, and backtrajectory cluster analysis, in: Proc. of SPIE Remote Sensing of Clouds and the Atmosphere XIX and Optics in Atmospheric Propagation and Adaptive Systems XVII, vol. 9242, edited by: Comerón, A., Kassianov, E. I., Schäfer, K., Picard, R. H., Stein, K., and Gonglewski, J. D., 92420F, doi:10.1117/12.2072049, 2014.

Banks, R. F., Tiana-Alsina, J., Rocadenbosch, F., and Baldasano, J. M.: Performance evaluation of boundary layer heights from lidar and the Weather Research and Forecasting model at an urban coastal site in the northeast Iberian Peninsula, Bound.-Lay. Meteorol., in press, 2015.

Basart, S., Pérez, C., Nickovic, S., Cuevas, E., Schulz, M., and Baldasano, J. M.: Development and evaluation of BSCDREAM8b dust regional model over Northern Africa, the Mediterranean and the Middle East regions, Tellus B, 64, 18539, doi:10.3402/tellusb.v64i0.18539, 2012.

Belegante, L., Bravo-Aranda, J. A., Freudenthaler, V., Nicolae, D., Talianu, C., Alados-Arboledas, L., Amodeo, A., Pappalardo, G., Engelmann, R., Baars, H., Wandinger, U., Papayannis, A., Kokkalis, P., and Pereira, S. N.: Experimental assessment of the lidar polarizing sensitivity in aerosol typing studies, Atmos. Meas. Tech. Discuss., in preparation, 2015.

Benedetti, A., Morcrette, J.-J., Boucher, O., Dethof, A., Engelen, R. J., Fisher, M., Flentje, H., Huneeus, N., Jones, L., Kaiser, J. W., Kinne, S., Mangold, A., Razinger, M., Simmons, A. J., and Suttie, M.: Aerosol analysis and forecast in the European Centre for Medium-Range Weather Forecasts Integrated Forecast System: 2. Data assimilation, J. Geophys. Res., 114, D13205, doi:10.1029/2008JD011115, 2009.

Binietoglou, I., Basart, S., Alados-Arboledas, L., Amiridis, V., Argyrouli, A., Baars, H., Baldasano, J. M., Balis, D., Belegante, L., Bravo-Aranda, J. A., Burlizzi, P., Carrasco, V., Chaikovsky, A., Comerón, A., D'Amico, G., Filioglou, M., Granados-Muñoz, M. J., Guerrero-Rascado, J. L., Ilic, L., Kokkalis, P., Maurizi, A., Mona, L., Monti, F., Muñoz-Porcar, C., Nicolae, D., Papayannis, A., Pappalardo, G., Pejanovic, G., Pereira, S. N., Perrone, M. R., Pietruczuk, A., Posyniak, M., Rocadenbosch, F., Rodríguez-Gómez, A., Sicard, M., Siomos, N., Szkop, A., Terradellas, E., Tsekeri, A., Vukovic, A., Wandinger, U., and Wagner, J.: A methodology for investigating dust model performance using synergistic EARLINET/AERONET dust concentration retrievals, Atmos. Meas. Tech. Discuss., 8, 3605–3666, doi:10.5194/amtd-8-3605-2015, 2015.

Böckmann, C., Wandinger, U., Ansmann, A., Bösenberg, J., Amiridis, V., Boselli, A., Delaval, A., De Tomasi, F., Frioud, M., Hågård, A., Horvat, M., Iarlori, M., Komguem, L. Kreipl, S., Larchevêque, G., Matthias, V., Papayannis, A., Pappalardo, G., Rocadembosch, F., Rodriguez, J. A., Schneider, J., Shcherbakov, V., and Wiegner, M.: Aerosol lidar intercomparison in the framework of the EARLINET project, 2. Aerosol backscatter algorithms, Appl. Optics, 43, 977–989, 2004.

Bösenberg, J., Ansmann, A., Baldasano, J. M., Balis, D., Böckmann, C., Calpini, B., Chaikovsky, A., Flamant, P., Hagard, A., Mitev, V., Papayannis, A., Pelon, J., Resendes, D., Schneider, J., Spinelli, N., Trickl, T., Vaughan, G., Visconti, G., and Wiegner, M.: EARLINET: a european aerosol research lidar network, in: Advances in Laser Remote Sensing, edited by: Dabas, A., Loth, C., and Pelon, J., Ecole polytechnique, Palaiseau CEDEX, France, 155–158, 2001.

Bravo-Aranda, J. A.: Lidar Depolarization Technique: Assessment of the Hardware Polarizing Sensitivity and Applications, PhD thesis, University of Granada, Department of Applied Physics, ISBN: 978-84-9083-080-2, available at: http://0-hera.ugr.es.adrastea.ugr.es/tesisugr/23799109.pdf, 2014.

Bravo-Aranda, J. A., Belegante, L., Freudenthaler, V., Alados-Arboledas, A., Nicolae, D., Amodeo, A., D'Amico, G., Engelmann, R., Kokkalis, P., Papayannis, A., and Wandinger, U.:

Assessment of lidar depolarization uncertainties by means of lidar polarizing sensitivity simulator, Atmos. Meas. Tech. Discuss., in preparation, 2015.
Burton, S. P., Ferrare, R. A., Hostetler, C. A., Hair, J. W., Rogers, R. R., Obland, M. D., Butler, C. F., Cook, A. L., Harper, D. B., and Froyd, K. D.: Aerosol classification using airborne High Spectral Resolution Lidar measurements – methodology and examples, Atmos. Meas. Tech., 5, 73–98, doi:10.5194/amt-5-73-2012, 2012.
Carnuth, W., Kempfer, U., and Trickl, T.: Highlights of the Tropospheric Lidar Studies at IFU within the TOR Project, Tellus B, 54, 163–185, 2002.
Chaikovsky, A., Dubovik, O., Goloub, P., Tanré, D., Pappalardo, G., Wandinger, U., Chaikovsky, A., Denisov, D., Grudo, Y., Lopatsin, A., Karol, Y., Lapyonok, T., Amiridis, V., Ansmann, A., Apituley, A., Alados-Arboledas, L., Binietoglou, I., Freudenthaler, V., Kokkalis, P., Granados Muñoz, M. J., Nicolae, D., Papayannis, A., Perrone, M. R., Pietruczuk, A., Pisani, G., Rocadenbosch, F., Sicard, M., Talianu, C., De Tomasi, F., Tsekeri, A., Wagner, J., and Wang, X.: Algorithm and software package for the retrieval of vertical aerosol properties in the atmospheric column using combined lidar/photometer data, Atmos. Meas. Tech. Discuss., in preparation, 2015.
Christensen, J. H.: The Danish Eulerian hemispheric model – a three-dimensional air pollution model used for the Arctic, Atmos. Environ., 31, 4169–4191, 1997.
Collins, W. D., Rasch, P. J., Eaton, B. E., Khattatov, B. V., and Lamarque, J.-F.: Simulating aerosols using a chemical transport model with assimilation of satellite aerosol retrievals: methodology for INDOEX, J. Geophys. Res., 106, 7313–7336, 2001.
Córdoba-Jabonero, C., Sorribas, M., Guerrero-Rascado, J. L., Adame, J. A., Hernández, Y., Lyamani, H., Cachorro, V., Gil, M., Alados-Arboledas, L., Cuevas, E., and de la Morena, B.: Synergetic monitoring of Saharan dust plumes and potential impact on surface: a case study of dust transport from Canary Islands to Iberian Peninsula, Atmos. Chem. Phys., 11, 3067–3091, doi:10.5194/acp-11-3067-2011, 2011.
D'Amico, G., Binietoglou, I., Amodeo, A., Pappalardo, G., Baars, H., Engelmann, R., Wandinger, U., Mattis, I., Freudenthaler, V., Wiegner, M., Nicolae, D., Chaikovsky, A., Apituley, A., and Adam, M.: EARLINET single calculus chain for automatic lidar data processing: first tests on optical products, in: Reviewed and Revised Papers Presented at the 26th International Laser Radar Conference (ILRC 2012), edited by: Papayannis, A., Balis, D., and Amiridis, V., 331–334, 2012.

AMTD
8, 6599–6659, 2015

D'Amico, G., Amodeo, A., Baars, H., Binietoglou, I., Freudenthaler, V., Mattis, I., Wandinger, U., and Pappalardo, G.: EARLINET Single Calculus Chain – general presentation, methodology and 5 strategy, Atmos. Meas. Tech. Discuss., 8, 4973–5023, doi:10.5194/amtd-8-4973-201, 2015a.
D'Amico, G., Amodeo, A., and Mattis, I.: Single Calculus Chain – technical Part 1: Preprocessing of raw lidar data, Atmos. Meas. Tech. Discuss., in preparation, 2015b.
Draxler, R. R. and Rolph, G. D.: NOAA AirResources Laboratory, Silver Spring, MD, available at: http://www.arl.noaa.gov/ready/hysplit4.html, 2003.
Dulac, F., Agacayak, T., Alados Arboledas, L., Alastuey, A., Ameur, Z., Ancellet, G., Assamoi, E.-M., Attié, J.-L., Becagli, S., Beekmann, M., Bergametti, G., Bocquet, M., Bordier, F., Bourrianne, T:, Chazette, P., Chiapello, I., Coddeville, P., Colomb, A., Comerón, A., D'Amico, G., D'Anna, B., Desboeufs, K., Descloitres, J., Diouri, M., Di Biagio, C., Di Sarra, G:, Durand, P., El Amraoui, L., Ellul, R., Fleury, L., Formenti, P., Freney, E., Gerasopoulos, E:, Goloub, P., Guerrero Rascado, J.-L., Guieu, C:, Hadjimitsis, D., Hamonou, E., Hansson, H. C., Iarlori, M., Ioannou, S., Jaumouillé, E., Jeannot, M., Junkermann, W., Keleshis, C., Kleanthous, S., Kokkalis, P., Lambert, D., Laurent, B., Léon, J.-F., Liousse, C., Lopez Bartolome, M., Losno, R., Mallet, M., Mamouri, R.-E., Marchand, N., Menut, L., Mihalopoulos, N., Morales Baquero, R., Nabat, P., Nicolae, D., Nicolas, J., Notton, G., Paoli, C., Papayannis, A., Pappalardo, G:, Pandis, S., Pelon, J., Pey, J., Pont, V., Querol, X., Ravetta, F., Renard, J.-B., Rizi, V., Roberts, G., Sartelet, K., Savelli, J.-L., Sciare, J., Sellegri, K:, Sferlazzo, D. M., Sicard, M., Smyth, A., Solmon, F., Tanré, D., Tovar Sánchez, A., Verdier, N., Wagner, F., Wang, Y., Wenger, J., and Yassaa, N.: An update on ChArMEx (the Chemistry-Aerosol Mediterranean Experiment) activities and plans for aerosol studies in the Mediterranean region, European Aerosol Conference, 2–7 September 2012, Granada, Spain, edited by: Alados Arboledas, L., and Olmo Reyes, F. J., 2012.
Engelmann, R., Guerrero Rascado, J. L., Alados Arboledas, L., Wandinguer, U., Freudenthaler, V., Baars, H., Mattis, I., Groß, S., Pappalardo, G., Amodeo, A., D'Amico, G., Giunta, A., Chaikovsky, A., Osipenko, F., Slesar, A., Nicolae, D., Belegante, L., Serikov, I., Linné, H., Jansen, F., Apituley, A., Wilson, K., Trickl, T., and Rocadenbosch, R.: Calibrated backscatter measurements at 1064 nm with lidar: techniques used in EARLINET and ACTRIS, Atmos. Meas. Tech. Discuss., in preparation, 2015.
Espen Yttri, K., Aas, W., Tørseth, K., Kristiansen, N. I., Lund Myhre, C., Tsyro, S., Simpson, D:, Bergström, R., Marečková, K., Wankmüller, R., Klimont, Z., Amman, M., Kouvarakis, G. N.,

Laj, P., Pappalardo, G., and Prévôt, A.: EMEP Co-operative Programme for Monitoring and Evaluation of the Long-Range Transmission of Air Pollutants in Europe, Transboundary particulate matter in Europe Status report 2012, available at: http://www.actris.net/Portals/97/documentation/dissemination/other/emep4-2012.pdf (last access: 9 December 2014), 2012.

Freudenthaler, V.: Polarization sensitivity of lidar systems and the 90°-calibration, Atmos. Meas. Tech. Discuss., in preparation, 2015.

Freudenthaler, V., Gross, S., Engelmann, R., Mattis, I., Wandinger, U., Pappalardo, G., Amodeo, A., Giunta, A., D'Amico, G:, Chaikovsky, A., Osipenko, F., Slesar, A., Nicolae, D., Belegante, L., Talianu, C., Serikov, I., Linne, H., Jansen, F., Wilson, K., de Graaf, M., Apituley, A., Trickl, T., Giehl, H., and Adam, M.: EARLI09 – direct intercomparison of eleven EARLINET lidar, in: Proc. of the 25th International Laser Radar Conference (ILRC), 891–894, 2010.

Freudenthaler, V., Linne, H., Chaikovski, A., Groß, S., and Rabus, D.: EARLINET lidar quality assurance tools, Atmos. Meas. Tech. Discuss., in preparation, 2015.

GAW Report No. 178: "Plan for the implementation of the GAW Aerosol Lidar Observation Network GALION", WMO/TD-No. 1443, 2007.

Granados-Muñoz, M. J., Navas-Guzmán, F., Guerrero-Rascado, J. L., Bravo-Aranda, J. A., Binietoglou, I., Pereira, S. N., Baldasano, J. M., Chaikovsky, A., Comerón, A., Belegante, L., D'Amico, G., Muñoz, C., Nicolae, D., Papayannis, A., Pappalardo, G., Rodríguez, A., Schepanski, K., Sicard, M., Wandinger, U., Olmo, F. J., and Alados-Arboledas, L., Profiles of aerosol microphysical properties during ChArMEx 2012 at European sites, Atmos. Chem. Phys. Discuss., in preparation, 2015.

Groß, S., Freudenthaler, V., Wiegner, M., Gasteiger, J., Geiß, A., and Schnell, F.: Dual-wavelength linear depolarization ratio of volcanic aerosols: lidar measurements of the Eyjafjallajökull plume over Maisach, Germany, Atmos. Environ., 48, 85–96, doi:10.1016/j.atmosenv.2011.06.017, 2011.

Guerrero-Rascado, J.-L., Ruiza, B., and Alados-Arboledas, L.: Multi-spectral Lidar characterization of the vertical structure of Saharan dust aerosol over southern Spain, Atmos. Environ., 42, 2668–2681, 2008.

Guerrero-Rascado, J. L., Olmo, F. J., Avilés-Rodríguez, I., Navas-Guzmán, F., Pérez-Ramírez, D., Lyamani, H., and Alados Arboledas, L.: Extreme Saharan dust event over the southern Iberian Peninsula in september 2007: active and passive remote sensing from surface and satellite, Atmos. Chem. Phys., 9, 8453–8469, doi:10.5194/acp-9-8453-2009, 2009.

AMTD
8, 6599–6659, 2015

Hoff, R. M., Bösenberg, J., and Pappalardo, G.: The GAW Aerosol Lidar Observation Network (GALION), International Geoscience and Remote Sensing Symposium (IGARSS-08), Boston, USA, 6–11 July 2008, 2008.
Holben, B., Eck, T. F., Slutsker, I., Tanré, D., Buis, J. P., Setzer, A., Vermote, E., Reagan, J. A., Kaufman, Y. J., Nakajima, T., Lavenu, F., Jankowiak, I., and Smirnov, A.: AERONET – a federated instrument network and data archive for aerosol characterization, Remote Sens. Environ., 66, 1–16, 1998.
IPCC: Chapter 7: clouds and aerosols, in: Climate Change 2013, The Physical Science Basis, Working Group I Contribution to the Fifth Assessment Report of the Intergovernmental Panel on Climate Change, edited by: Stocker, T. F., Qin, D., Plattner, G.-K., Tignor, M., Allen, S. K., Doschung, J., Nauels, A., Xia, Y., Bex, V., and Midgley, P. M., Cambridge University Press, New York, 571–658, doi:10.1017/CBO9781107415324.016, 2014.
Landulfo, E., Papayannis, A., Artaxo, P., Castanho, A. D. A., de Freitas, A. Z., Souza, R. F., Vieira Junior, N. D., Jorge, M. P. M. P., Sánchez-Ccoyllo, O. R., and Moreira, D. S.: Synergetic measurements of aerosols over São Paulo, Brazil using LIDAR, sunphotometer and satellite data during the dry season, Atmos. Chem. Phys., 3, 1523–1539, doi:10.5194/acp-3-1523-2003, 2003.
Mallet, V., Quélo, D., Sportisse, B., Ahmed de Biasi, M., Debry, É., Korsakissok, I., Wu, L., Roustan, Y., Sartelet, K., Tombette, M., and Foudhil, H.: Technical Note: The air quality modeling system Polyphemus, Atmos. Chem. Phys., 7, 5479–5487, doi:10.5194/acp-7-5479-2007, 2007.
Mamouri, R. E., Amiridis, V., Papayannis, A., Giannakaki, E., Tsaknakis, G., and Balis, D. S.: Validation of CALIPSO space-borne-derived attenuated backscatter coefficient profiles using a ground-based lidar in Athens, Greece, Atmos. Meas. Tech., 2, 513–522, doi:10.5194/amt-2-513-2009, 2009.
Mamouri, R. E., Ansmann, A., Nisantzi, A., Kokkalis, P., Schwarz, A., and Hadjimitsis, D.: Low Arabian dust extinction-to-backscatter ratio, Geophys. Res. Lett., 40, 4762–4766, doi:10.1002/grl.50898, 2013.
Matthias, V., Bösenberg, J., Freudenthaler, V., Amodeo, A., Balis, D., Chaikovsky, A., Chourdakis, G., Comeron, A., Delaval, A., de Tomasi, F., Eixmann, R., Hågård, A., Komguem, L., Kreipl, S., Matthey, R., Mattis, I., Rizi, V., Rodriguez, J. A., Simeonov, V., and Wang, X.: Aerosol lidar intercomparison in the framework of the EARLINET project, 1. Instruments, Appl. Optics, 43, 961–976, 2004.

AMTD
8, 6599–6659, 2015

Mattis, I., Siefert, P., Müller, D., Tesche, M., Hiebsch, A., Kanitz, T., Schmidt, J., Finger, F., Wandinger, U., and Ansmann, A.: Volcanic aerosol layers observed with multiwavelength Raman lidar over central Europe in 2008–2009, J. Geophys. Res., 115, D00L04, doi:10.1029/2009JD013472, 2010.
Mattis, I., Madonna, F., D'Amico, G., Amodeo, A., and Baars, H.: EARLINET-ASOS Single Calculus Chain technical Part 2: Calculation of optical products, Atmos. Meas. Tech. Discuss., in preparation, 2015.
Molero, F., Sicard, M., Navas-Guzmán, F., Preißler, J., Amodeo, A., Freudenthaler, V., Fernandez, A. J., Tomas, S., Granados, M. J., Wagner, F., Giunta, A., Mattis, I., Pujadas, M., Comeron, A., Alados-Arboledas, L., Guerrero-Rascado, J. L., D'Amico, G., Lange, D., Bravo, J. A., Kumar, D., Pappalardo, G., Giner, J., Muñoz, C., and Rocadenbosch, F.: Study on aerosol properties over Madrid (Spain) by multiple instrumentation during SPALI10 lidar campaign, Óptica Pura y Aplicada, 45, 405–413, 2012.
Mona, L., Amodeo, A., Pandolfi, M., and Pappalardo, G.: Saharan dust intrusions in the Mediterranean area: three years of Raman lidar measurements, J. Geophys. Res., 111, D16203, doi:10.1029/2005JD006569, 2006.
Mona, L., Pappalardo, G., Amodeo, A., D'Amico, G., Madonna, F., Boselli, A., Giunta, A., Russo, F., and Cuomo, V.: One year of CNR-IMAA multi-wavelength Raman lidar measurements in coincidence with CALIPSO overpasses: Level 1 products comparison, Atmos. Chem. Phys., 9, 7213–7228, doi:10.5194/acp-9-7213-2009, 2009.
Mona, L., Papagiannopoulos, N., Basart, S., Baldasano, J., Binietoglou, I., Cornacchia, C., and Pappalardo, G.: EARLINET dust observations vs. BSC-DREAM8b modeled profiles: 12-year-long systematic comparison at Potenza, Italy, Atmos. Chem. Phys., 14, 8781–8793, doi:10.5194/acp-14-8781-2014, 2014.
Müller, D., Mattis, I., Ansmann, A., Wandinger, U., Ritter, C., and Kaiser, D.: Multiwavelength Raman lidar observations of particle growth during long-range transport of forest-fire smoke in the free trosposphere, Geophys. Res. Lett., 34, L05803, doi:10.1029/2006GL027936, 2007a.
Müller, D., Ansmann, A., Mattis, I., Tesche, M., Wandinger, U., Althausen, D., and Pisani, G.: Aerosol-type-dependent lidar ratios observed with Raman lidar, J. Geophys. Res., 112, D16202, doi:10.1029/2006JD008292, 2007b.
Nabat, P., Somot, S., Mallet, M., Michou, M., Sevault, F., Driouech, F., Meloni, D., di Sarra, A., Di Biagio, C., Formenti, P., Sicard, M., Léon, J.-F., and Bouin, M.-N.: Dust aerosol radiative

effects during summer 2012 simulated with a coupled regional aerosol–atmosphere–ocean model over the Mediterranean, Atmos. Chem. Phys., 15, 3303–3326, doi:10.5194/acp-15-3303-2015, 2015.

Navas-Guzmán, F., Müller, D., Bravo-Aranda, J. A., Guerrero- Rascado, J. L., Granados-Muñoz, M. J., Pérez-Ramírez, D., Olmo, F. J., and Alados-Arboledas, L.: Eruption of the Eyjafjallajökull Volcano in spring 2010: multiwavelength raman lidar measurements of sulfate particles in the lower troposphere, J. Geophys. Res., 118, 1804–1813, doi:10.1002/jgrd.50116, 2013.

Nickovic, S., Papadopoulos, A., Kakaliagou, O., and Kallos, G.: A model for prediction of desert dust cycle in the atmosphere. J. Geophys. Res., 106, 18113–18129, 2001.

Nicolae, D., Nemuc, A., Müller, D., Talianu, C., Vasilescu, J., Belegante, L., and Kolgotin, A.: Characterization of fresh and aged biomass burning events using multiwavelength Raman lidar and mass spectrometry, J. Geophys. Res.-Atmos., 118, 2956–2965, doi:10.1002/jgrd.50324, 2013.

Nisantzi, A., Mamouri, R. E., Ansmann, A., and Hadjimitsis, D.: Injection of mineral dust into the free troposphere during fire events observed with polarization lidar at Limassol, Cyprus, Atmos. Chem. Phys., 14, 12155–12165, doi:10.5194/acp-14-12155-2014, 2014.

Nisantzi, A., Mamouri, R. E., Ansmann, A., Schuster, G. L., and Hadjimitsis, D. G.: Middle East versus Saharan dust extinction-to-backscatter ratios, Atmos. Chem. Phys. Discuss., 15, 5203–5240, doi:10.5194/acpd-15-5203-2015, 2015.

Papayannis, A., Amiridis, V., Mona, L., Tsaknakis, G., Balis, D., Bösenberg, J., Chaikovski, A., De Tomasi, F., Grigorov, I., Mattis, I., Mitev, V., Müller, D., Nickovic, S., Pérez, C., Pietruczuk, A., Pisani, G., Ravetta, F., Rizi, V., Sicard, M., Trickl, T., Wiegner, M., Gerding, M., Mamouri, R. E., D'Amico, G., and Pappalardo, G.: Systematic lidar observations of Saharan dust over Europe in the frame of EARLINET (2000–2002), J. Geophys. Res., 113, D10204, doi:10.1029/2007JD009028, 2008.

Papayannis, A., Mamouri, R. E., Amiridis, V., Giannakaki, E., Veselovskii, I., Kokkalis, P., Tsaknakis, G., Balis, D., Kristiansen, N. I., Stohl, A., Korenskiy, M., Allakhverdiev, K., Huseyinoglu, M. F., and Baykara, T.: Optical properties and vertical extension of aged ash layers over the Eastern Mediterranean as observed by Raman lidars during the Eyjafjallajökull eruption in May 2010, Atmos. Environ., 48, 56–65, doi:10.1016/j.atmosenv.2011.08.037, 2012.

Pappalardo, G., Amodeo, A., Mona, L., Pandolfi, M., Pergola, N., and Cuomo, V.: Raman lidar observations of aerosol emitted during the 2002 Etna eruption, Geophys. Res. Lett., 31, L05120, doi:10.1029/2003GL019073, 2004a.
Pappalardo, G., Amodeo, A., Pandolfi, M., Wandinger, U., Ansmann, A., Bosenberg, J., Matthias, V., Amiridis, V., De Tomasi, F., Frioud, M., Iarlori, M., Komguem, L., Papayannis, A., Rocadenbosch, F., and Wang, X.: Aerosol lidar intercomparison in the framework of the EARLINET project, 3. Raman lidar algorithm for aerosol extinction, backscatter and lidar ratio, Appl. Optics, 43, 5370–5385, 2004b.
Pappalardo, G., Papayannis, A., Bösenberg, J., Ansmann, A., Apituley, A., Alados Arboledas, L., Balis, D., Böckmann, C., Chaikovsky, A., Comeron, A., Gustafsson, O., Hansen, G., Mitev, V., Mona, L., Nicolae, D., Perrone, M. R., Pietruczuk, A., Pujadas, M., Putaud, J.-P., Ravetta, F., Rizi, F., Simeonov, V., Spinelli, N., Stoyanov, D., Trickl, T., and Wiegner, M.: EARLINET coordinated lidar observations of Saharan dust events on continental scale, IOP C. Ser. Earth Env., 7, 1, doi:10.1088/1755-1307/7/1/012002, 2009.
Pappalardo, G., Wandinger, U., Mona, L., Hiebsch, A., Mattis, I., Amodeo, A., Ansmann, A., Seifert, P., Linne, H., Apituley, A., Alados Arboledas, L., Balis, D., Chaikovsky, A., D'Amico, G., De Tomasi, F., Freudenthaler, V., Giannakaki, E., Giunta, A., Grigorov, I., Iarlori, M., Madonna, F., Mamouri, R.-E., Nasti, L., Papayannis, A., Pietruczuk, A., Pujadas, M., Rizi, V., Rocadenbosch, F., Russo, F., Schnell, F., Spinelli, N., Wang, X., and Wiegner, M.: EARLINET correlative measurements for CALIPSO: first intercomparison results, J. Geophys. Res., 115, D00H19, doi:10.1029/2009JD012147, 2010.
Pappalardo, G., Mona, L., D'Amico, G., Wandinger, U., Adam, M., Amodeo, A., Ansmann, A., Apituley, A., Alados Arboledas, L., Balis, D., Boselli, A., Bravo-Aranda, J. A., Chaikovsky, A., Comeron, A., Cuesta, J., De Tomasi, F., Freudenthaler, V., Gausa, M., Giannakaki, E., Giehl, H., Giunta, A., Grigorov, I., Groß, S., Haeffelin, M., Hiebsch, A., Iarlori, M., Lange, D., Linné, H., Madonna, F., Mattis, I., Mamouri, R.-E., McAuliffe, M. A. P., Mitev, V., Molero, F., Navas-Guzman, F., Nicolae, D., Papayannis, A., Perrone, M. R., Pietras, C., Pietruczuk, A., Pisani, G., Preißler, J., Pujadas, M., Rizi, V., Ruth, A. A., Schmidt, J., Schnell, F., Seifert, P., Serikov, I., Sicard, M., Simeonov, V., Spinelli, N., Stebel, K., Tesche, M., Trickl, T., Wang, X., Wagner, F., Wiegner, M., and Wilson, K. M.: Four-dimensional distribution of the 2010 Eyjafjallajökull volcanic cloud over Europe observed by EARLINET, Atmos. Chem. Phys., 13, 4429–4450, doi:10.5194/acp-13-4429-2013, 2013.

AMTD
8, 6599–6659, 2015

Pappalardo, G., Amodeo, A., Apituley, A., Comeron, A., Freudenthaler, V., Linné, H., Ansmann, A., Bösenberg, J., D'Amico, G., Mattis, I., Mona, L., Wandinger, U., Amiridis, V., Alados-Arboledas, L., Nicolae, D., and Wiegner, M.: EARLINET: towards an advanced sustainable European aerosol lidar network, Atmos. Meas. Tech., 7, 2389–2409, doi:10.5194/amt-7-2389-2014, 2014.
Pérez, C., Nickovic, S., Baldasano, J. M., Sicard, M., Rocadenbosch, F., and Cachorro, V. E.: A long Saharan dust event over the western Mediterranean: lidar, sun photometer observations, and regional dust modeling, J, Geophys. Res., 111, D15214, doi:10.1029/2005JD006579, 2006a.
Pérez, C., Nickovic, S., Pejanovic, G., Baldasano, J. M., and Ozsoy, E.: Interactive dust-radiation modeling: a step to improve weather forecasts, J. Geophys. Res., 111, D16206, 1–17, doi:10.1029/2005JD006717, 2006b.
Pey, J., Querol, X., Alastuey, A., Forastiere, F., and Stafoggia, M.: African dust outbreaks over the Mediterranean Basin during 2001–2011: PM_{10} concentrations, phenomenology and trends, and its relation with synoptic and mesoscale meteorology, Atmos. Chem. Phys., 13, 1395–1410, doi:10.5194/acp-13-1395-2013, 2013.
Rasch, P. J., Collins, W. D., and Eaton, B. E.: Understanding the Indian Ocean Experiment (INDOEX) aerosol distributions with an aerosol assimilation, J. Geophys. Res., 106, 7337–7355, 2001.
Reba, M. N. M., Rocadenbosch, F., Sicard, M., Kumar, D., and Tomás, S.: On the lidar ratio estimation from the synergy between AERONET sun-photometer data and elastic lidar inversion, in: Proc. of the 25th International Laser Radar Conference, vol. 2, ISBN 978-5-94458-109-9, Saint-Petersburg (Rusia), 5–9 July 2010, 1102–1105, 2010.
Rolph, G. D.: NOAA Air Resources Laboratory, Silver Spring, MD, available at: http://www.arl.noaa.gov/ready/hysplit4.html, 2003.
Roustan, Y., Sartelet, K. N., Tombette, M., Debry, E., and Sportisse, B.: Simulation of aerosols and gas-phase species over Europe with the POLYPHEMUS system, Part II: Model sensitivity analysis for 2001, Atmos. Environ., 44, 4219–4229, 2010.
Sartelet, K. N., Debry, E., Fahey, K. M., Roustan, Y., Tombette, M., and Sportisse, B.: Simulation of aerosols and gas-phase species over Europe with the Polyphemus system, Part I: Model-to-data comparison for 2001, Atmos. Environ., 29, 6116–6131, 2007.
Sicard, M., Molero, F., Guerrero-Rascado, J. L., Pedrós, R., Expósito, F. J., Córdoba-Jabonero, C., Bolarín, J. M., Comerón, A., Rocadenbosch, F., Pujadas, M., Alados-

AMTD
8, 6599–6659, 2015

Arboledas, L., Martinez-Lozano, J. A., Díaz, J. P., Gil, M., Requena, A., Navas-Guzmán, F., and Moreno, J. M.: Aerosol lidar intercomparison in the framework of SPALINET – the SPAnish LIdar NETwork: methodology and results, IEEE T. Geosci. Remote, 47, 3547–3559, 2009.
Sicard, M., Rocadenbosch, F., Reba, M. N. M., Comerón, A., Tomás, S., García-Vízcaino, D., Batet, O., Barrios, R., Kumar, D., and Baldasano, J. M.: Seasonal variability of aerosol optical properties observed by means of a Raman lidar at an EARLINET site over Northeastern Spain, Atmos. Chem. Phys., 11, 175–190, doi:10.5194/acp-11-175-2011, 2011.
Sicard, M., Guerrero-Rascado, J. L., Navas-Guzmán, F., Preißler, J., Molero, F., Tomás, S., Bravo-Aranda, J. A., Comerón, A., Rocadenbosch, F., Wagner, F., Pujadas, M., and Alados-Arboledas, L.: Monitoring of the Eyjafjallajökull volcanic aerosol plume over the Iberian Peninsula by means of four EARLINET lidar stations, Atmos. Chem. Phys., 12, 3115–3130, doi:10.5194/acp-12-3115-2012, 2012.
The EARLINET publishing group 2000–2010: EARLINET correlative observations for CALIPSO (2006–2010), World Data Center for Climate (WDCC), doi:10.1594/WDCC/EN_Calipso_2006-2010, 2014.
Tombette, M., Mallet, V., and Sportisse, B.: PM_{10} data assimilation over Europe with the optimal interpolation method, Atmos. Chem. Phys., 9, 57–70, doi:10.5194/acp-9-57-2009, 2009.
Tsyro, S., Schulz, M., Mona, L., and Aas, W.: Regional and global calculations of mineral dust with the EMEP model, in: International Conference on Atmospheric Dust – DUST 2014, 425 pp., Castellaneta Marina (TA), Italy, 1–6 June 2014, 2014.
Vukovic, A., Mona, L., Vujadinovic, M., Nickovic, S., Pejanovic, G., Cvetkovic, B., Djordjevic, M., D'amico, G., Papagiannopoulos, N., and Pappalardo, G.: Application of lidar observations in atmospheric dust transport forecast, in: International Conference on Atmospheric Dust – DUST 2014, Castellaneta Marina (TA), Italy, 1–6 June 2014, 2014.
Wagner, J., Ansmann, A., Wandinger, U., Seifert, P., Schwarz, A., Tesche, M., Chaikovsky, A., and Dubovik, O.: Evaluation of the Lidar/Radiometer Inversion Code (LIRIC) to determine microphysical properties of volcanic and desert dust, Atmos. Meas. Tech., 6, 1707–1724, doi:10.5194/amt-6-1707-2013, 2013.
Wandinger, U., Hiebsch, A., Mattis, I., Pappalardo, G., Mona, L., and Madonna, F.: Aerosols and Clouds: Long-Term Database From Spaceborne Lidar Measurements, ESTEC Contract 21487/08/NL/HE, Final Report, 2011.

AMTD
8, 6599–6659, 2015

EARLINET: potential operationality of a research network

M. Sicard et al.

Wandinger, U., Freudenthaler, V., Baars, H., Amodeo, A., Engelmann, R., Mattis, I., Groß, S., Pappalardo, G., Giunta, A., D'Amico, G., Chaikovsky, A., Osipenko, F., Slesar, A., Nicolae, D., Belegante, L., Talianu, C., Serikov, I., Linné, H., Jansen, F., Apituley, A., Wilson, K., de Graaf, M., Trickl, T., Giehl, H., Adam, M., Comeron, A., Rocadenbosch, F., Sicard, M., Pujadas, M., Molero, F., Alados-Arboledas, L., Preißler, J., Wagner, F., Pereira, S., Lahnor, B., Gausa, M., Grigorev, I., Stoyanov, D., Iarlori, M., and Rizi, V.: EARLINET instrument intercomparison campaigns: overview on strategy and results, Atmos. Meas. Tech. Discuss., in preparation, 2015.

Wang, X., Boselli, A., D'Avino, L., Pisani, G., Spinelli, N., Amodeo, A., Chaikovsky, A., Wiegner, M., Nickovic, S., Papayannis, A., Perrone, M. R., Rizi, V., Sauvage, L., and Stohl, A.: Volcanic dust characterization by EARLINET during Etna's eruptions in 2001–2002, Atmos. Environ., 42, 893–905, 2008.

Wang, Y., Sartelet, K. N., Bocquet, M., Chazette, P., Sicard, M., D'Amico, G., Léon, J. F., Alados-Arboledas, L., Amodeo, A., Augustin, P., Bach, J., Belegante, L., Binietoglou, I., Bush, X., Comerón, A., Delbarre, H., García-Vízcaino, D., Guerrero-Rascado, J. L., Hervo, M., Iarlori, M., Kokkalis, P., Lange, D., Molero, F., Montoux, N., Muñoz, A., Muñoz, C., Nicolae, D., Papayannis, A., Pappalardo, G., Preissler, J., Rizi, V., Rocadenbosch, F., Sellegri, K., Wagner, F., and Dulac, F.: Assimilation of lidar signals: application to aerosol forecasting in the western Mediterranean basin, Atmos. Chem. Phys., 14, 12031–12053, doi:10.5194/acp-14-12031-2014, 2014.

AMTD
8, 6599–6659, 2015
EARLINET: potential operationality of a research network
M. Sicard et al.

Table 1. Wavelengths and temporal resolution, Δt, of the systems involved in the exercise.

Station	Elastic wavelengths (nm)								Raman wavelengths (nm)					Δt (s)
	351	355			532			1064	382	387	393	408	607	
		Total	//[1]	⊥[2]	Total	//[1]	⊥[2]							
EV		x			x		x	x		x			x	30
MA		x			x			x		x			x	60
GR		x				x	x	x		x		x	x	60
BA		x			x			x		x		x	x	60
CL			x	x						x		x		60
PA		x								x		x		60
LA	x								x		x			300
PO		x				x	x	x		x			x	60
AT		x	x	x	x			x		x		x	x	60
BU		x				x	x	x		x		x	x	60 d / 300 n[3]
LM						x	x	x					x	48

[1] // indicates the parallel polarization component wrt the laser polarization. [2] ⊥ indicates the perpendicular polarization component wrt the laser polarization. [3] d indicates day and n night.

AMTD
8, 6599–6659, 2015

Table 2. Number of files at the different stages of the exercise and finally inverted by the SCC.

Files expected	$N = 720$			
Files received by the SCC	$N_{SCC} = 662$ (92 % wrt N)			
Files processed successfully by ELPP	$N_{ELPP} = 648$ (98 % wrt N_{SCC})			
Files processed successfully by ELDA	$N_{ELDA} = 555$ (84 % wrt N_{SCC}; 86 % wrt N_{ELPP})			
Wavelength (nm)	351	355	532	1064
e files	25	164	172	–
b files	57	440	452	452

Discussion Paper | Discussion Paper | Discussion Paper | Discussion Paper |

AMTD
8, 6599–6659, 2015

EARLINET: potential operationality of a research network

M. Sicard et al.

Figure 1. Geographical position of the eleven stations that participated in the exercise. Green labels indicate advanced lidar systems; orange labels indicate Raman lidar systems. Yellow circles indicate co-located sun-photometers.

AMTD
8, 6599–6659, 2015

EARLINET: potential operationality of a research network

M. Sicard et al.

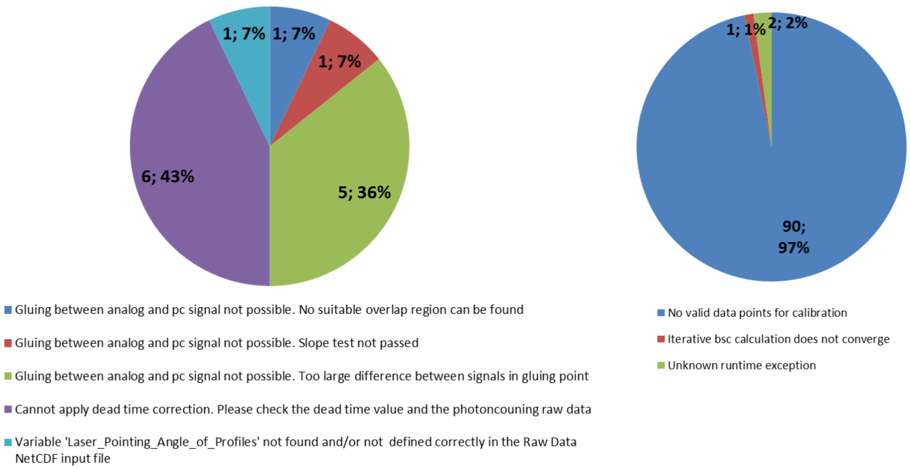

Figure 2. Number and frequency (in %) of the reasons for which either the pre-processing (ELPP, left) or the optical processing (ELDA, right) could not derive a solution. The color legend indicates the error code.

AMTD
8, 6599–6659, 2015

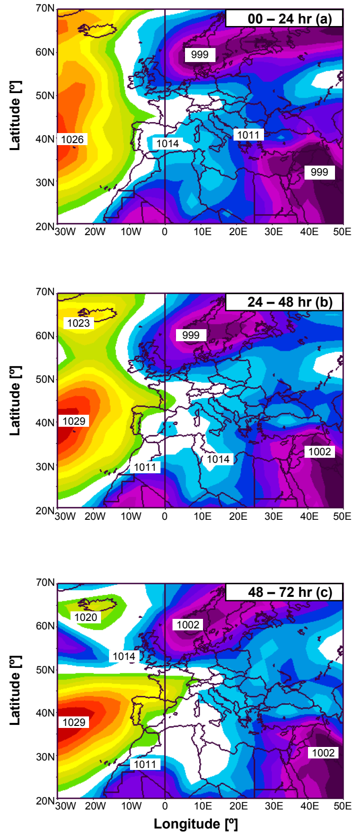

Figure 3. Mean synoptic situation from the NCEP/NCAR Reanalysis project at **(a)** 00–24, **(b)** 24–48 and **(f)** 48–72 h after the “GO”. Purple and red colors represent low and high pressures, respectively.

AMTD

8, 6599–6659, 2015

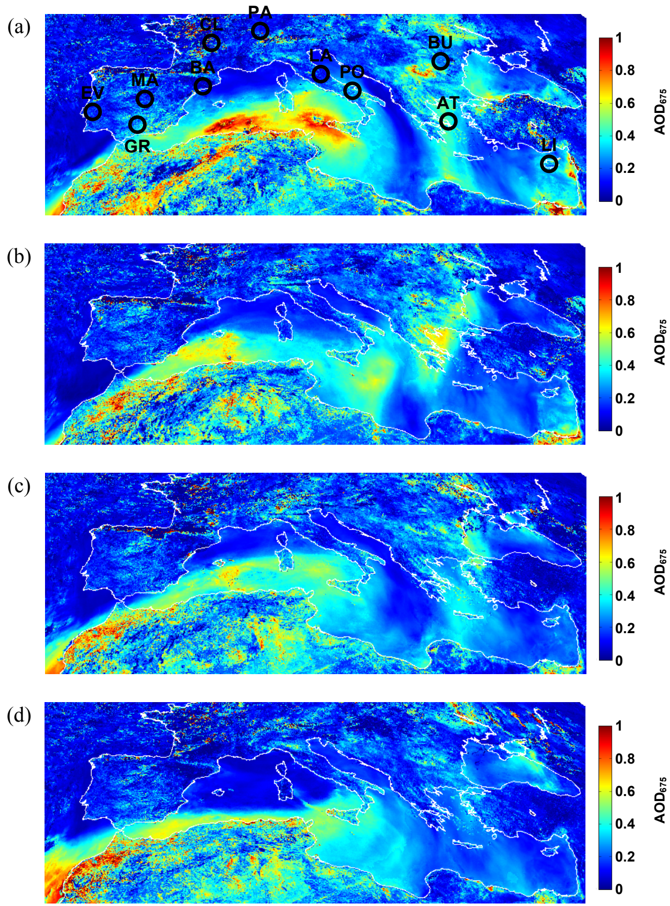

Figure 4. MSG/SEVIRI AERUS-GEO daily AOD at 675 nm on **(a)** J09, **(b)** J10, **(c)** J11 and **(d)** J12.

AMTD
8, 6599–6659, 2015

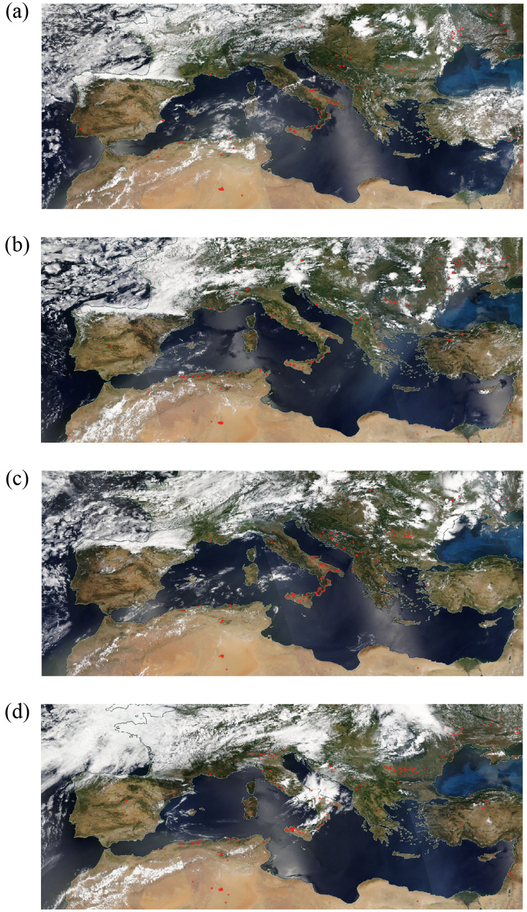

Figure 5. Aqua/and Terra/MODIS fire overlays on **(a)** J09, **(b)** J10, **(c)** J11 and **(d)** J12 from https://earthdata.nasa.gov/labs/worldview/.

AMTD
8, 6599–6659, 2015

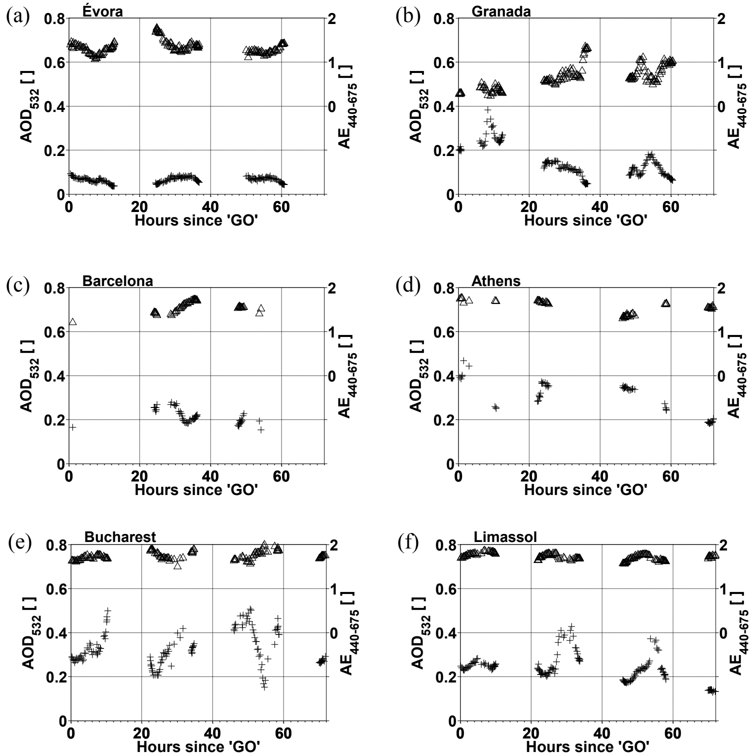

Figure 6. Sun-photometer AOD at 532 nm (crosses, left axis) and the Ångström exponent calculated between the wavelengths at 440 and 675 nm (triangles, right axis) from AERONET level 2.0 data at **(a)** Évora, **(b)** Granada, **(c)** Barcelona, **(d)** Athens, **(e)** Bucharest and **(f)** Limassol. Clouds were present at Clermont-Ferrand. No data are available in Potenza during the period.

AMTD
8, 6599–6659, 2015

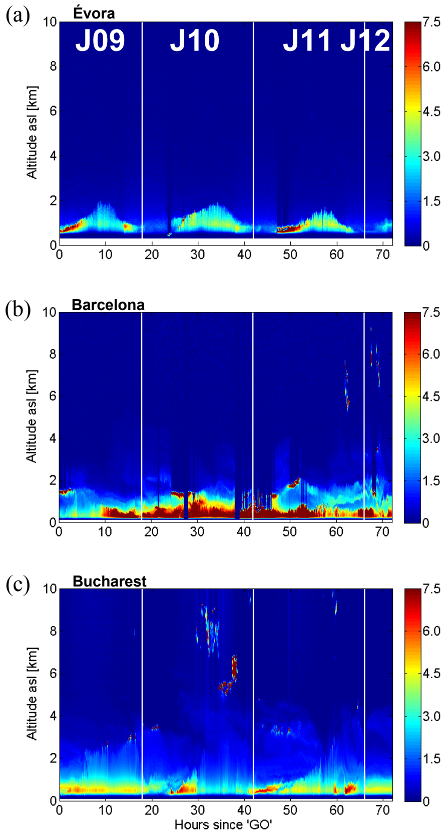

Figure 7. Quicklooks of the attenuated backscatter not corrected for the total transmissivity [a. u.] at 1064 nm in **(a)** Évora, **(b)** Barcelona and **(c)** Bucharest. The white vertical lines indicate a change in the date. The attenuated backscatter is not a product of the SCC.

AMTD
8, 6599–6659, 2015

EARLINET: potential operationality of a research network

M. Sicard et al.

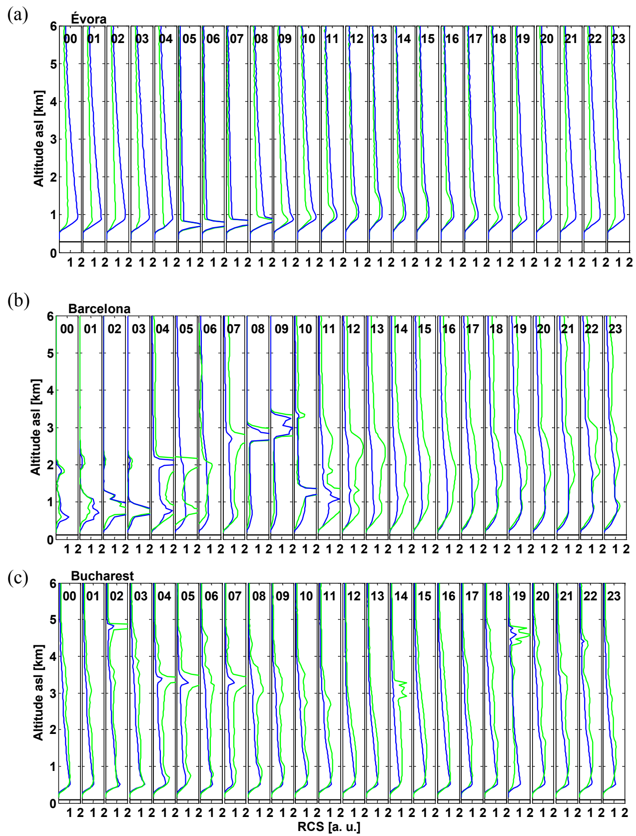

Figure 8. 24 h evolution of the hourly RCS profiles (SCC-1 product) at 355 (blue lines) and 532 nm (green lines) on J11 in **(a)** Évora, **(b)** Barcelona and **(c)** Bucharest. The numbers in the top of the plots indicate the time in UT. The horizontal black lines represent the station's altitude a.s.l.

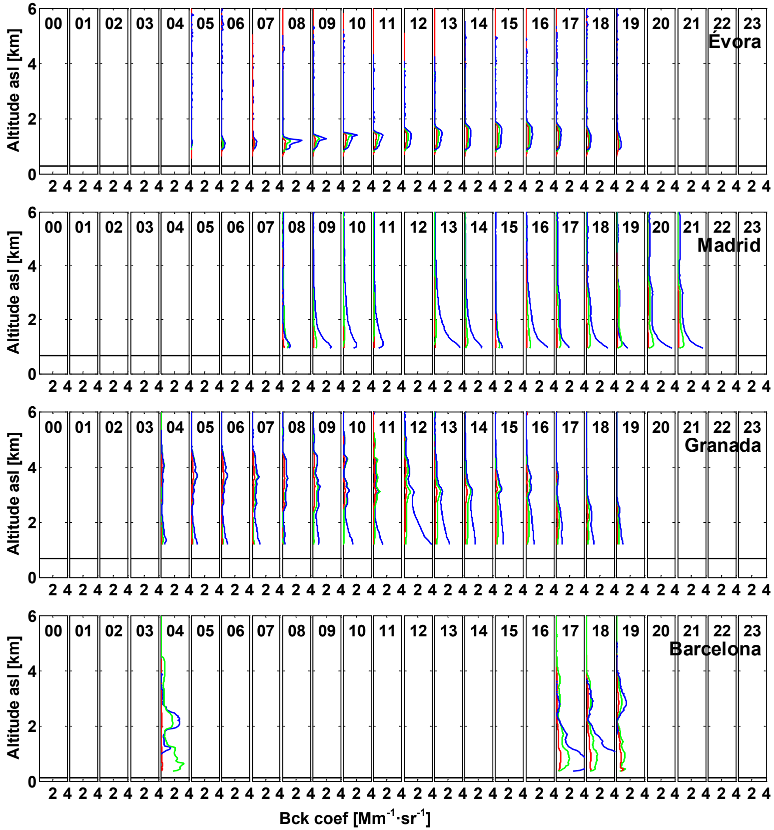

Figure 9. Time series of elastic-inverted backscatter coefficient profiles (SCC-2 product) on J10 at 355 (blue), 532 nm (green) and 1064 nm (red) at the Iberian stations ordered west to east. The numbers below the top axis indicate the time in UT. The horizontal black lines represent the station's altitude a.s.l.

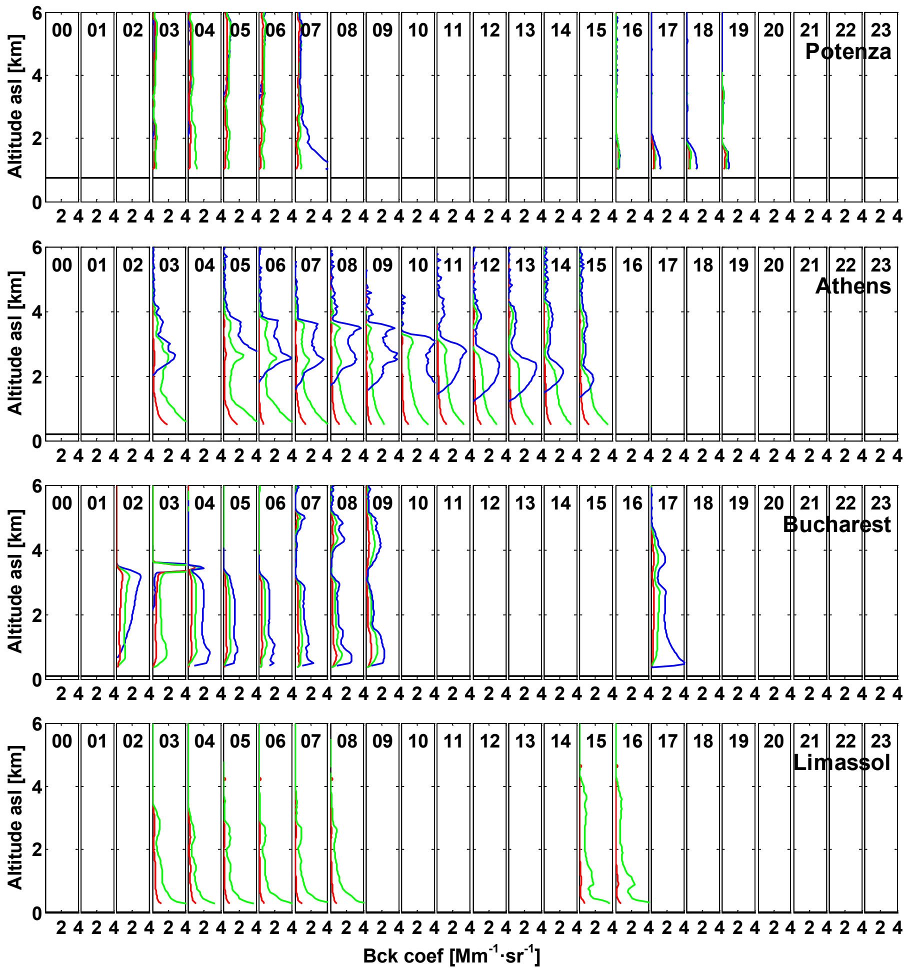

Figure 10. Idem as Fig. 9 at the central and eastern European stations ordered west to east.

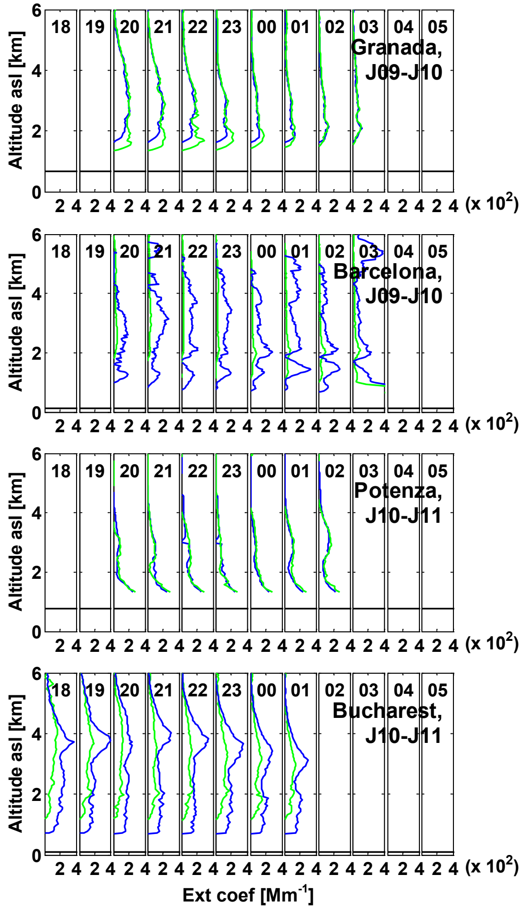

Figure 11. Time series of Raman-inverted extinction coefficient profiles (SCC-2 product) at 355 (blue) and 532 nm (green). The numbers below the top axis indicate the time in UT. The horizontal black lines represent the station's altitude a.s.l.

AMTD
8, 6599–6659, 2015

EARLINET: potential operationality of a research network

M. Sicard et al.

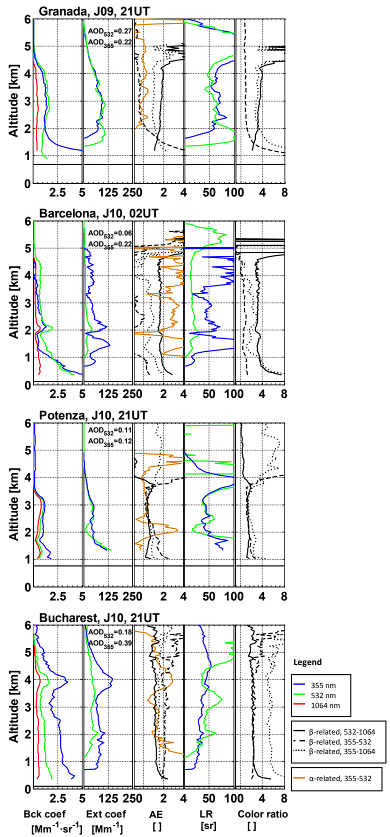

Figure 12. All optical products (SCC-2 direct and derived products) at a selected time. The legend is the same for all the plots and is reported in the bottom right corner. The values of AOD_{532} and AOD_{355} in the extinction coefficient plots refer to the integral of the extinction coefficient profiles at 532 and 355 nm, respectively. The horizontal black lines represent the station's altitude a.s.l.

AMTD
8, 6599–6659, 2015

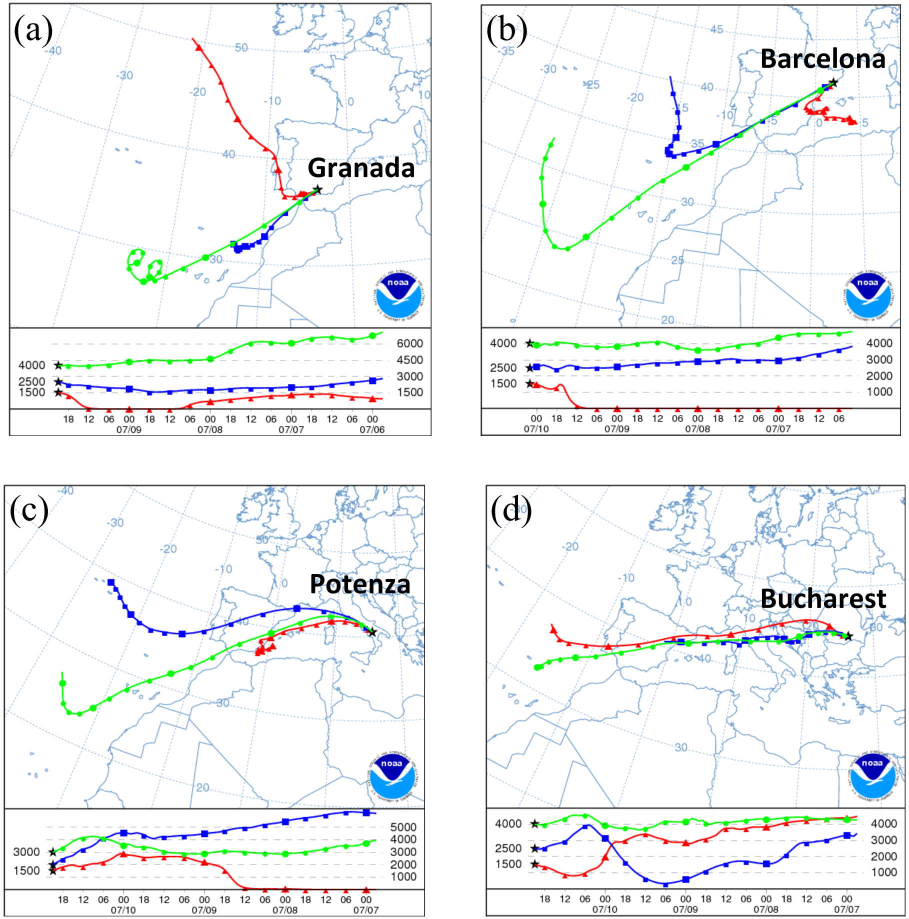

Figure 13. HYSPLIT 4 day backtrajectories **(a)** in Granada on J09 at 21:00 UT, **(b)** in Barcelona on J10 at 02:00 UT, **(c)** in Potenza on J10 at 21:00 UT and **(d)** in Bucharest on J10 at 21:00 UT.

AMTD
8, 6599–6659, 2015